#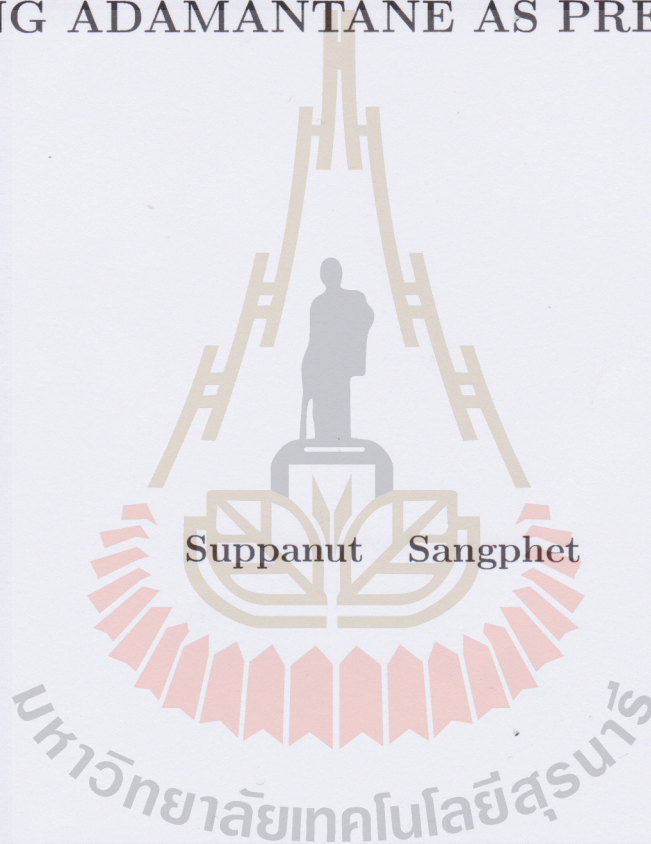 STUDY OF ORIGIN AND ENHANCEMENT OF ROOM- TEMPERATURE FERROMAGNETISM IN CVD- CARBON FILMS PREPARED BY USING ADAMANTANE AS PRECURSOR

Suppanut   Sangphet

A Thesis Submitted in Partial Fulfillment of the Requirements for the

Degree of Master of Science in Physics

Suranaree University of Technology

Academic Year 2016

การศึกษาแหล่งกำเนิดและการทำให้เพิ่มขึ้นของคุณสมบัติเฟอร์โรแมกเนติกที่
อุณหภูมิห้องในฟิล์มคาร์บอนที่เตรียมโดยใช้อะดาเมนเทนเป็นสารตั้งต้น

นายศุภณัฐ สังข์เพ็ชร
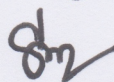
STUDY OF ORIGIN AND ENHANCEMENT OF ROOM-TEMPERATURE FERROMAGNETISM IN CVD-CARBON FILMS PREPARED BY USING ADAMANTANE AS PRECURSOR
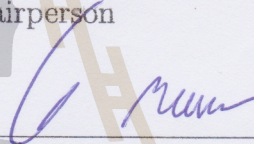
Suranaree University of Technology has approved this thesis submitted in partial fulfillment of the requirements for a Master's Degree.
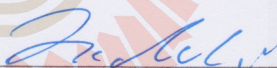
Thesis Examining Committee

_____
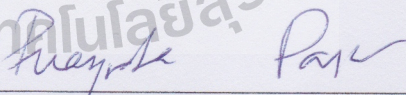
(Prof. Dr. Santi Maensiri)

Chairperson

_____

(Asst. Prof. Dr. Worawat Meevasana)

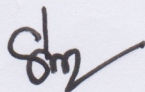Member (Thesis Advisor)

_____

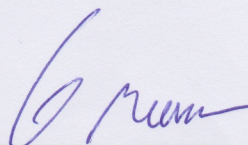(Dr. Hideki Nakajima)

Member

_____

(Assoc. Prof. Dr. Puangratana Pairor)

Member

_____

(Prof. Dr. Santi Maensiri)

Vice Rector for Academic Affairs

and Internationalization

_____

(Asst. Prof. Dr. Worawat Meevasana)

Dean of Institute of Science

ศุภณัฐ สังข์เพ็ชร : การศึกษาแหล่งกำเนิดและการทำให้เพิ่มขึ้นของคุณสมบัติเฟอร์โรแมก
เนติกที่อุณหภูมิห้องในฟิล์มคาร์บอนที่เตรียมโดยใช้อะดาเมนเทนเป็นสารตั้งต้น (STUDY
OF ORIGIN AND ENHANCEMENT OF ROOM-TEMPERATURE
FERROMAGNETISM IN CVD-CARBON FILMS PREPARED BY USING
ADAMANTANE AS PRECURSOR). อาจารย์ที่ปรึกษา : ผู้ช่วยศาสตราจารย์ ดร.วรวัฒน์
มีวาสนา, 54 หน้า.

วัสดุเฟอร์โรแมกเนติกโดยทั่วไปจะประกอบด้วยธาตุโลหะที่มีอิเล็กตรอนในชั้น d และ f
บรรจุแบบไม่เต็ม อาทิ เหล็ก นิกเกิล และ โคบอลต์ เป็นต้น ปัจจุบันได้มีการศึกษาวัสดุเฟอร์โรแมก
เนติกและนำไปประยุกต์อย่างกว้างขวาง อย่างไรก็ตาม มีการค้นพบว่าวัสดุคาร์บอน สามารถแสดง
คุณสมบัติเฟอร์โรแมกเนติกที่อุณหภูมิห้องได้ เช่น กราไฟต์ และ C60 และเมื่อไม่นานมานี้ คุณ
สมบัติเฟอร์โรแมกเนติกยังสามารถพบในเทปลอน และพาราฟิล์ม ได้อีกด้วย

ในการศึกษาครั้งนี้ ได้พบคุณสมบัติเฟอร์โรแมกเนติกที่อุณหภูมิห้องของฟิล์มคาร์บอนที่
เตรียมโดยใช้อะดาเมนเทนเป็นสารตั้งต้น อะดาเมนเทนเป็นโมเลกุลที่มีขนาดเล็กที่สุดของวัสดุ
ไฮโดรคาร์บอนที่มีโครงสร้างคล้ายเพชรที่เรียกว่าไดมอนดอยด์ โดยฟิล์มคาร์บอนของข้าพเจ้าที่ถูก
เตรียมด้วยเทคนิคการเคลือบด้วยไอเคมี (chemical vapor deposition) แสดงคุณสมบัติเฟอร์โรแมก
เนติกที่มีค่าอิ่มตัวของแมกเนไทเซชันประมาณ 6.2 emu•cm^{-3} ผลการวิเคราะห์องค์ประกอบธาตุของ
วัสดุด้วยเทคนิควิเคราะห์ธาตุเชิงพลังงานพบว่าไม่มีธาตุแม่เหล็ก (เช่น เหล็ก นิกเกิล และ โคบอลต์)
ในปริมาณที่มากพอที่จะส่งผลต่อค่าแมกเนไทเซชัน จึงเป็นการยืนยันว่าสามารถสร้างวัสดุที่มี
คุณสมบัติเฟอร์โรแมกเนติกจากคาร์บอนได้ด้วยวิธีการเคลือบด้วยไอเคมี นอกจากนี้ยังสามารถเพิ่ม
ค่าการอิ่มตัวของแมกเนไทเซชันในฟิล์มคาร์บอนด้วยการใช้การสอกฟิล์ม ซึ่งได้ค่าแมกเนไทเซชัน
เพิ่มขึ้นประมาณ 8.4 เท่า ในส่วนของการศึกษาแหล่งกำเนิดของคุณสมบัติเฟอร์โรแมกเนติกนั้น รา
มานสเปกตรัมแสดงถึงพันธะคาร์บอน sp^2 sp^3 และพันธะ C-H ที่พบในฟิล์มคาร์บอน ดังนั้น
คุณสมบัติเฟอร์โรแมกเนติกในฟิล์มคาร์บอนอาจจะเกิดมาจากพันธะคาร์บอนที่ไม่สมบูรณ์ หรือที่
เรียกว่า dangling bond

สาขาวิชาฟิสิกส์   ลายมือชื่อนักศึกษา _____

ปีการศึกษา 2559   ลายมือชื่ออาจารย์ที่ปรึกษา _____

SUPPANUT SANGPHET : STUDY OF ORIGIN AND
ENHANCEMENT OF ROOM-TEMPERATURE FERROMAGNETISM
IN CVD-CARBON FILMS PREPARED BY USING ADAMANTANE
AS PRECURSOR. THESIS ADVISOR : ASST. PROF.
WORAWAT MEEVASANA, Ph.D. 54 PP.

ADAMANTANE/ RAMAN SPECTROSCOPY/ FERROMAGNETISM/
DANGLING BOND

Conventional ferromagnetic materials usually contain metal elements whose d- or f-orbital is incompletely filled (e.g. iron, nickel, and cobalt). However, it was found that carbon-based materials can exhibit ferromagnetism such as fullerene(C_{60}), carbon nanotube, and disordered graphite. The most recent room-temperature ferromagnetism were unexpectedly found in carbon-compounds materials such as Teflon and Parafilm.

In this work, room-temperature ferromagnetism was discovered in carbon films prepared by using adamantane: the smallest member of the so-called diamondoid series (a hydrocarbon material which has cage structure like diamond). These carbon films that were prepared by operating chemical vapor deposition technique exhibited ferromagnetic signal with moderately strong saturated magnetization as large as $6.2 \ emu \cdot cm^{-3}$. By using energy dispersive x-ray spectroscopy, there are no evidences of magnetic elements such as Fe, Co, and Ni. Therefore, this suggests an inexpensive method in creating magnetic carbon nano-materials and magnetic-media coating. Intriguingly, ferromagnetic signal in our CVD-carbon film could be further enhanced after mechanical exfoliation; its saturation magnetization could be enhanced by 8.4 times. To explain the ferromagnetism observation, Raman

spectrum revealed the mixture of carbon bondings in CVD-carbon film, including of sp^2, sp^3, and C-H types. These suggest that during CVD-process, the dangling bonds may be the cause of ferromagnetism. Moreover, dangling bond would more align in the same direction after exfoliation, resulting the enhancement of ferromagnetism

School of Physics

Academic Year 2016

Student's Signature _____

Advisor's Signature _____

ACKNOWLEDGEMENTS

My thesis could not have been completed without many great help and support from many people. In the first and foremost, I would like to express my utmost gratitude to my advior, Asst. Prof. Dr. Worawat Meevasana. It has been such a great experience working with him since my second year of bachelor degree. Almost 3 years, this is valuable times that I join in Meevasana group. I recognize and appreciate all of his supports and encouragements not only in research works but also life skills; for example, he gave me a big chance to join international conferences at China and USA and also international in Thailand as NanoThailand 2017, for presenting my work since the first year of master degree. In these places I will learn new aspects research and make my wider world. His great attitude towards all dimensions in life. Furthermore, I have learn great behavior from my advisor, i.e. leadership and good teamwork. With his super kindness and excellent abilities, I feel like I am one of the luckiest student under his supervision.

I would like to thank Prof. Dr. Santi Maensiri, the Dean of Institute of Science who supports furnace to create all CVD-carbon film. He always gives good views not only for research working, but also for other activities. With this, I learn experienced skills that make I can work together to people.

I would like to thank Assoc. Prof. Dr. Supree Pinitsoontorn and Miss Nipaporn Sriplai from the Department of Physics, Khon Kean university, who have kindly taught me to operate a vibrating sample magnetometer. Without their help, we would have not been able to neither measure the magnetic property nor find ferromagnetism in CVD-carbon films, which is the main part in our work.

In Meevasana's group, I would like to thank P' S who taught me how to

prepare CVD-carbon film and always gives me a great help, and my friend Chart, who supported and worked together with me for at least 2 years. I would like to thank other members in Meevasana's group who always support me and give good relationships.

I would like to thank Dr. Nakajima, P' Noom, and P' Au the operators at BL3.2a (SLRI) for their expertise in X-ray photoemission spectroscopy and their kindness.

I would like to thanks all teachers, staffs (especially P'Khae) and students in the School of Physics, Institute of Science, SUT, for all kindly supporting me.

I also would like to thank the Development and Promotion of Science and Technology Talent Project (DPST) for financial support since I studied at bachelor's degree.

My friends of the first generation of Physics SUT and other friends who always support me in every kinds of work.

Last and most importantly, I would like to thank my parents for who always give me loving, supporting and encouraging words to me.

Suppanut Sangphet

CONTENTS

CONTENTS (Continued)

LIST OF FIGURES

LIST OF FIGURES (Continued)

LIST OF FIGURES (Continued)

LIST OF FIGURES (Continued)

LIST OF FIGURES (Continued)

LIST OF FIGURES (Continued)

CHAPTER I

INTRODUCTION

1.1 Motivation

Ferromagnetic materials and their applications have been widely studied for a long times. It is known that ferromagnets usually compose of metal elements whose d- or f-orbital is incompletely filled. Iron, nickel, and cobalt are the most well-known examples. Ferromagnetic materials have played important roles in advanced technologies, such as in magnetic shielding, hard disk applications and drug delivery which uses magnetic nano particles for storing and transporting. However, there are some limitations such as heavy weight, not flexible and quite expensive. To overcome these limitations, carbon possibly is one of the candidates. Carbon based materials can be ferromagnetic. Ferromagnetism in graphite was first reported in 2002 by Esquinazi et al (Esquinazi et al., 2002). One year later, the same group (Esquinazi et al.) reported a finding ferromagnetic behavior in proton-irradiated highly oriented pyrolytic graphite (HOPG), whose saturated magnetization is around 3.5×10^{-5} emu (Esquinazi et al., 2003). This report has inspired other scientists to study ferromagnetism in other carbon based materials including graphite (Han et al., 2003; Ohldag et al., 2007; Xia et al., 2008; Yang et al., 2009), graphene (Wang et al., 2009; Ugeda et al., 2010), fullerene (C60) (Makarova et al., 2001; Wood et al., 2002), carbon nanotube (Zanolli and Charlier, 2010; Friedman et al., 2010), nano-diamond (Talapatra et al., 2005) and other free-metal materials (Coey, 2005; Saito et al., 2011). Recently, there are studies of ferromagnetism created in polymers such as Teflon (Ma et al., 2012) and

Parafilm (Sriplai et al., 2015). Interesting view from these polymers studies are sample preparations. They all used simple method such as cutting, stretching, and annealing for creating ferromagnetic behavior.

In my senior project, I studied magnetic behaviors of carbon film prepared by using chemical vapor deposition (CVD) technique, operated at 1,050 °C. We used nano hydrocarbon called adamantane as a precursor. It is the smallest member of nano hydro-carbon called "diamondoid" which has cage structure like diamond. We found our carbon film has a saturation magnetization approximately is 6.2 $emu \cdot cm^{-3}$ at room-temperature. We checked that ferromagnetic signal does not cause by metal impurities such as Fe, Ni, and Co. However the origin of our ferromagnetism is still unclear.

1.2 Outline of Thesis

This thesis is divided into five chapters. In the Chapter II, I will introduce the background knowledge of diamondoid and adamantane (the smallest member of diamondoid) which is used as a precursor for creating my carbon films. The simple models of carbon hybridizations as sp^2 and sp^3 and chemical vapor deposition (CVD) technique that is used to prepare our carbon films are also presented in this chapter. Furthermore, scanning electron microscopy (SEM), energy dispersive x-ray spectroscopy (EDS) and Raman spectroscopy used to study the carbon structure will be included. In Chapter III, background studies about ferromagnetic property in carbon based materials, the growth techniques, and the proposed origins of ferromagnetism will be presented. Magnetic properties, including ferromagnetism, diamagnetism, and paramagnetism are also included. Magnetic measurement technique as vibrating sample magnetometer (VSM) and hysteresis loop section which is widely used to study magnetic phenomena are described in

the last part of chapter III. In chapter IV, all the results are shown. Physical observations of our CVD-carbon films were first reported. Ferromagnetic properties in the CVD-film and chemical characterizations, including energy dispersive spectroscopy and x-ray photoemission spectroscopy, are then shown. After that the study of origin and the enhancement of ferromagnetism by using mechanical exfoliation and light irradiation will be presented, respectively. For the last chapter V, summary and future direction of our work will be described.

CHAPTER II

CVD-ADAMANTANE FILM

By using chemical vapor deposition technique, we created carbon film by using the so-called adamantane as a precursor; adamantane is the smallest member of saturated nano-hydrocarbon material of nano-series of diamondoid. Therefore, in this chapter, firstly I will provide an introduction of diamondoid series and adamantane that was used as precursor to create our CVD-carbon films. Some basic knowledges about diamond-like-carbon material related to our films will be given as well. The films preparation by using chemical vapor deposition (CVD) technique and their characterizations will be included in section 2.3.

2.1 Diamondoid

Diamondoids are one type of carbon which are cage-like, highly stable, saturated nano-hydrocarbon. These consist of carbon-carbon bonding which has a number of six-member carbon fused together in ring-shape (known as cyclo-hexamantane) and carbon-hydrogen bonding terminated, followed by the formula $C_{4n+6}H_{4n+12}$ (see Figure 2.1) (Mansoori, 2007). Since their carbon are only sp^3 structure and constitute periodic repeating unit of diamond lattice structure, therefore diamondoids are very stable compounds. The simplest and smallest diamondoid is the so called adamantane which will be given more details in following section. Diamondoids are naturally found in crude oils (petroleum deposits). Diamondoids have been of a great interest in recent years due to their individual structures that mix together between hydrocarbon molecules and nano-sized di-

amond lattice. Recently, they are found outstanding properties of diamondoid monolayer as ultra-low effective work function (Narasimha et al., 2016) and the so called negative electron affinity effect (Yang et al., 2007); the vacuum level is below the conduction band maximum making electron can be released at low kinetic energy. With these properties, diamondoids have efficient potential to be used as electron-emitting device and electrode for solar cell. Moreover, due to their exceptional cage structures, they can play a role in nanotechnology and medicine applications, e.g. drug-delivery and DNA-direct assembly (Ramezani and Mansoori, 2007; George et al., 2007).
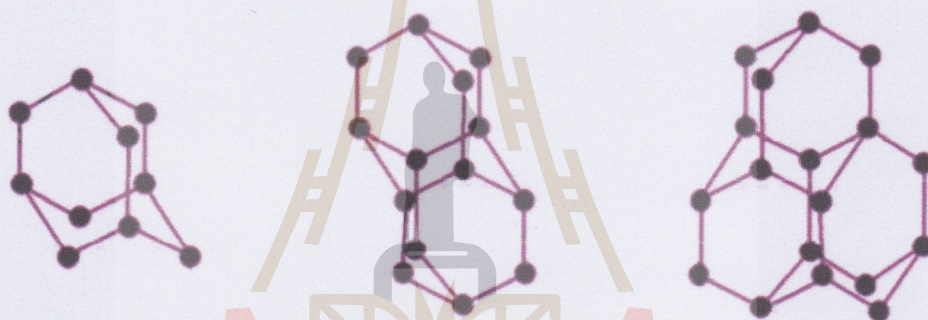
Figure 2.1 Molecular structures of diamondoid series, including adamantane ($C_{10}H_{16}$), diamantane ($C_{14}H_{20}$), and trimantane ($C_{18}H_{24}$) (Mansoori, 2007).

2.1.1 Adamantane

Adamantane is the smallest member of the diamondoids series, represented in chemical formula as $C_{10}H_{16}$. It is a tri-cyclic saturated hydrocarbon compounds where each cyclic consists of six carbon molecules as shown in Figure 2.2. It has been found that adamantane assembles in a crystal face-centered cubic lattice which is not normally found for an organic compound. This therefore makes it a very strong and stable compound. Like other members of diamondoids se-

ries, it has been found the notable properties of these series as negative electron affinity (Meevasana et al., 2009). Currently, adamantane has been used as counter electrode in dye-sensitized solar cells (DSSCs), see the manuscript in (Siriroj et al., 2016), and may also find applications in other devices such as perovskite solar cell, batteries, and supercapacitors.
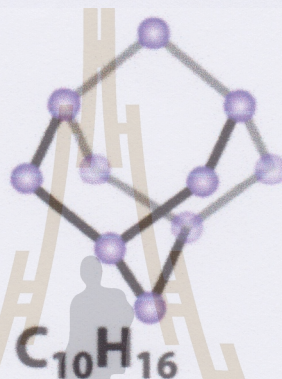
Figure 2.2 Adamantane, $C_{10}H_{16}$ (Meevasana et al., 2009).

2.2 Diamond like carbon

Diamond like carbon (DLC) is an unique type of amorphous carbon exhibiting some natural properties of diamond. It contains the significant amount of sp^3 hybridization carbon bonding. It was firstly unexpectedly discovered in 1971 during the study on diamond preparation. Currently, scientists can prepare DLC compounds by using various methods, based on deposition process, such as chemical vapor deposition (CVD), physical vapor deposition (PVD) and sputtering/plasma composite method (Robertson, 2002; Moriguchi et al., 2016). Due to their structures, it can have interesting properties, such as high mechanical hardness and optical transparency. DLC compounds have a possible ability to apply in

widespread applications, e.g. magnetic protective coating, biomedical coating and micro-electromechanical devices (MEMs).

2.2.1 Carbon hybridizations

It has been known that carbon has several allotropes including crystalline and disordered structures because its valence electrons can arrange and typically bond with each others in various ways called hybridization. There are three types: sp, sp^2 and sp^3 hybridizations. Generally, at ground state, valence electron configuration of a carbon atom consists of 2 electrons at s-orbital and 2 electrons from p-orbital (Figure 2.3). The illustrates unoccupied p-type orbitals indicate the possibilities to be new bondings. In sp^3 configuration, as in diamond, one electron in s-orbital is rearranged to be available p-orbitals and three electron p-orbitals form with the last electron at valence s-orbital, leading to four sp^3 hybridizations. This allows four strong σ bonds, demonstrating why diamond is a strong tetrahedral lattice (see in Figure 2.4). In three-hand sp^2 hybridization as found in graphite, two of three 2p-orbital electrons form together with an electron at 2s-orbital, causing the three σ bonds, arranging in triangle planar shape. And the third of 2p atom forms in weak π bond with an neighbouring atom as shown in Figure 2.5. While, in sp configuration, only a 2p- electron bond to the 2s electron, forming a σ bond, and other valence electrons form with σ bond.

2.3 Carbon films preparation

As mentioned, CVD-carbon films were prepared by using chemical vapor deposition technique and they exhibited unique physical view. In this section, therefore I will introduce an essential concept of chemical vapor deposition technique, scanning electron microscopy and related technique used to characterize
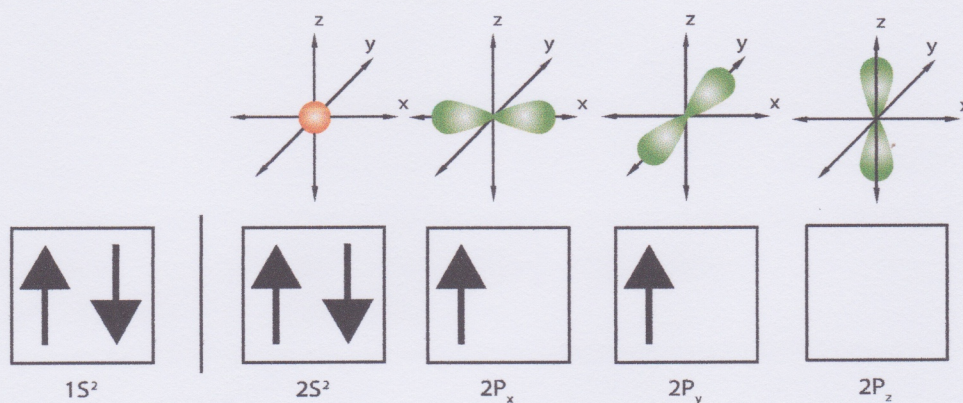
Figure 2.3 Electron configuration and its orbital shapes of carbon atom at ground state. At the valance shell, they have 2 s-electrons and 2 p-electrons
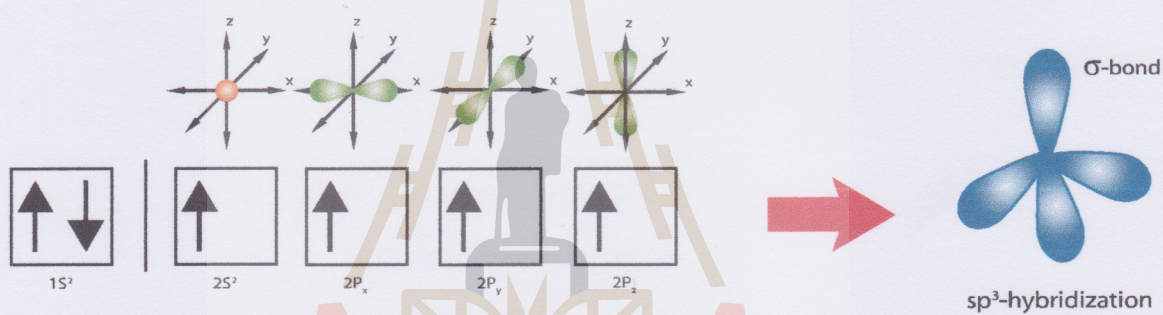
Figure 2.4 Electron configuration and the orbital shape of sp^3-hybridizations carbon atom.
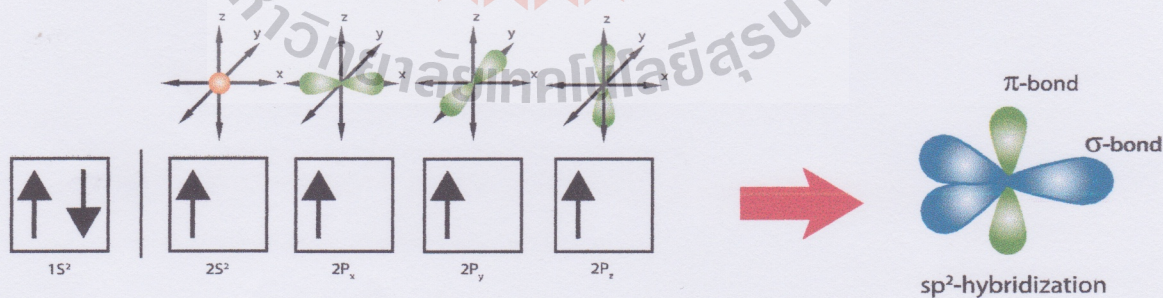
Figure 2.5 Electron configuration and the orbital shape of sp^2 hybridizations of carbon atom.

these films. The films preparation and some characters of the CVD-carbon films will be included.

2.3.1 Chemical vapor deposition technique

Chemical vapor deposition is a famous deposition technique used to create both purity and amorphous films. Unlike physical vapor deposition, materials used to be precursor in chemical vapor deposition technique is in a gas phase. In CVD-process, substrate was first annealed before in order to make active surface ready to be coated on. Then evaporated precursor was transported into substrate's chamber and disorderly formed on the active substrate's surface. Purity of CVD-film depends on several parameters, including substrate's temperature, quality of atmosphere, and active surface site of substrate.

In our CVD system, the films were prepared on various substrates, that is, quartz(SiO_2), sapphire, silicon, sand and rice husks. The substrates were ultrasonically cleaned in ethanol and placed on a holder inside a furnace. Vacuum pump was applied to our CVD-system in order to make clean atmosphere inside the substrate chamber, as shown the schematic of the CVD-system in Figure 2.6. The furnace was pumped out to a pressure of around 10^{-5} torr and then argon gas was flowed in for cleaning up the CVD system before operating. The precursor (adamantane powder) was placed in a separate chamber. During the deposition, the precursor and substrate chambers were heated to 90 °C and 1,050 °C, respectively.

2.3.2 Scanning electron microscopy (SEM)

Scanning electron microscopy (SEM) is a famous and powerful technique used to investigate physical properties of material. Its focused beam of high-
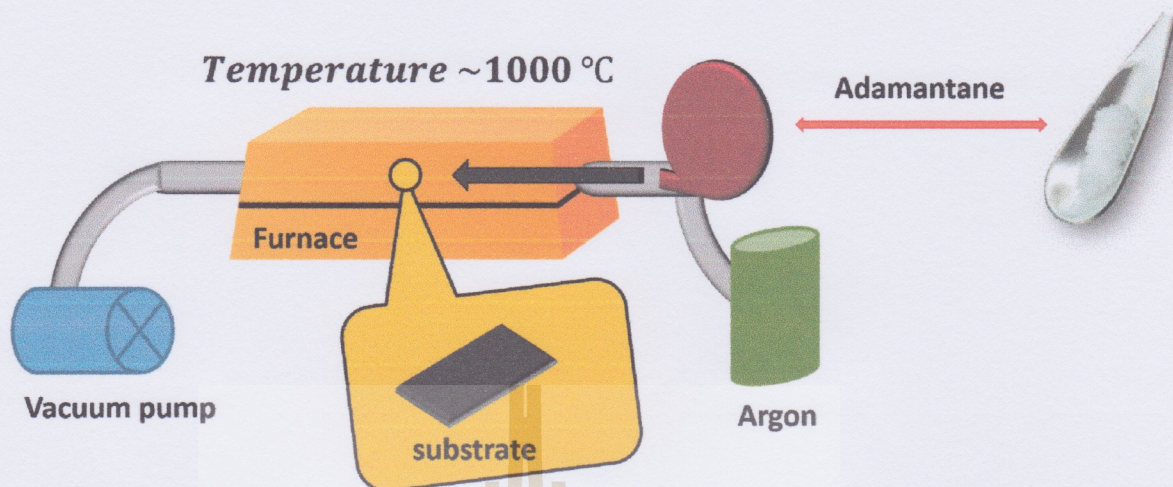
Figure 2.6 Schematic diagram of our the chemical vapor deposition (CVD) system.

intensity electron is shined on the sample to produce surface image of a sample. The incident electrons interact with atom in the solid sample and provide a variety of electron signals that contain significant information about sample's topography and chemical composition. These types of signals created by SEM include secondary electron (SE) (that is related to SEM image), backscattered electrons (BSE), photon or characteristic x-rays (that is used to investigate chemical deposition), visible light, absorb current, transmitted electrons, and heat. These signals are originated from the interaction between electron beam and atom at various depths location within sample. Secondary electrons and backscattered electron are principally used for imaging. In secondary imaging, due to the location of their productions that are very close to the sample surface, therefore, SE are most valuable signal for occurring topography and morphology image of sample. Regarding BSE, they are reflected from sample by elastic scattering. Although their resolutions is less than SE, however, BSE is another important signal used to create SEM image. BSE, made in from characteristic x-rays, contain information for

illustrating the contrast or the distribution of different compositions in sample. In the view of sample preparation, SEM's sample should have to resist to vacuum condition and high energy beam. The higher electrical conductivity should work on measuring SEM because nonconductive specimen will collect charge when shining electron beam, causing charging. Currently, with rising of high technology, SEM is able to observe the selected position; this function allow us to determine chemical composition (using energy dispersive x-ray spectroscopy, EDS), crystalline pattern and orientations.

In our work, we operated SEM measurements by using high resolution SEM (ZIESS, Auriga), with a voltage of 10 kV, organized by The Center for Scientific and Technological Equipment (CSTE), Suranaree University of Technology.
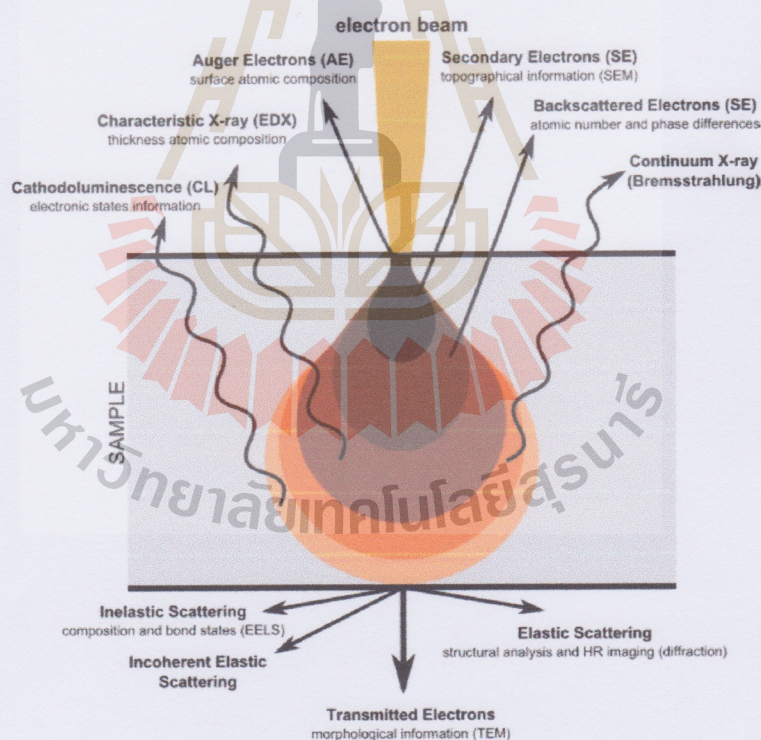
Figure 2.7 Electron-sample interaction in SEM process.

2.3.3 Energy dispersive X-ray spectroscopy (EDS)

Energy dispersive X-ray spectroscopy (EDS) is an analytical technique used for chemical analysis. With using high intensity of electron source, EDS technique can accurately probe localized chemical elements. To produce emission of characteristic X-ray signal from testing material, a high-intensity of electron beam is shined on sample(see in Figure 2.8). The incident electron beam may excite electron in core level, creating electron hole where electron was. The characteristic X-ray of different energy of moving electron from a higher energy level to the lower one can be expressed in X-ray form, which can be detected by energy dispersive spectrometer. Regarding to the limitation and accuracy, usually EDS cannot measure the light elements (i.e. H, He, ad Li) and its detection limits are typically about 1000 ppm (by weight) but it can be improved by measuring long counting times. Due to the electron source which is similar to be used in scanning electron microscopy(SEM), currently there is considerable overlap between SEM and EDS techniques. In this objective, therefore SEM can be used for electron mapping, and even point chemical analysis.

2.4 Raman spectroscopy

Raman spectroscopy is most commonly used technique for investigating carbon bondings in materials. This technique is inelastic light scattering, observed vibrational mode and other low-frequency modes. Generally, Raman spectroscopy uses monochromatic light source (i.e. laser of visible light) for exposing on the surface sample and detects absorbed light. The shining laser interacts with both molecules and molecular vibrations (phonon) and other excitations in surface and inside sample, indicating the energy shifted laser. The majority of scattered light
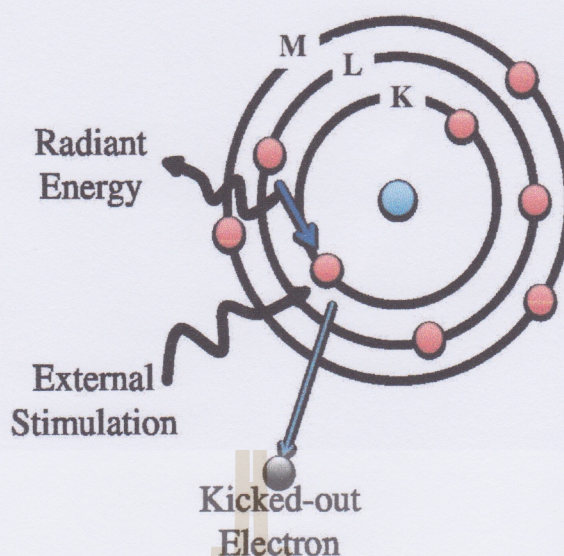
Figure 2.8 Schematic diagram of energy dispersive x-ray spectroscopy (EDS). Incident electron beam excites core-level electron, leaving an vacancy which is filled by electron from higher level, emitting the characteristic x-ray.

has the same frequency of incident source called Rayleigh or elastic scattering light. While inelastic scattered light is the resulting laser that has energy either lower and higher energy than incoming laser. This minority of inelastic scattered photon is result of Raman spectroscopy. Typically, sample measured in Raman should be a solid. Raman spectroscopy provides several benefits; it can be operated at normal atmospheric pressure and could be detected low frequency signal such as sulfur bond and carbon bond which infrared spectroscopy cannot be detected. Moreover, both organic and inorganic materials can also be measured.

In this work, all Raman measurements were performed by using dispersive Raman spectroscopy organized by Synchrotron Light Research Institute (SLRI), Nakhon Ratchasima. Green laser of 523 nanometer was used as a light source through the measurements. Figure 2.9 shows an example of raman spectra of adamantane powder.
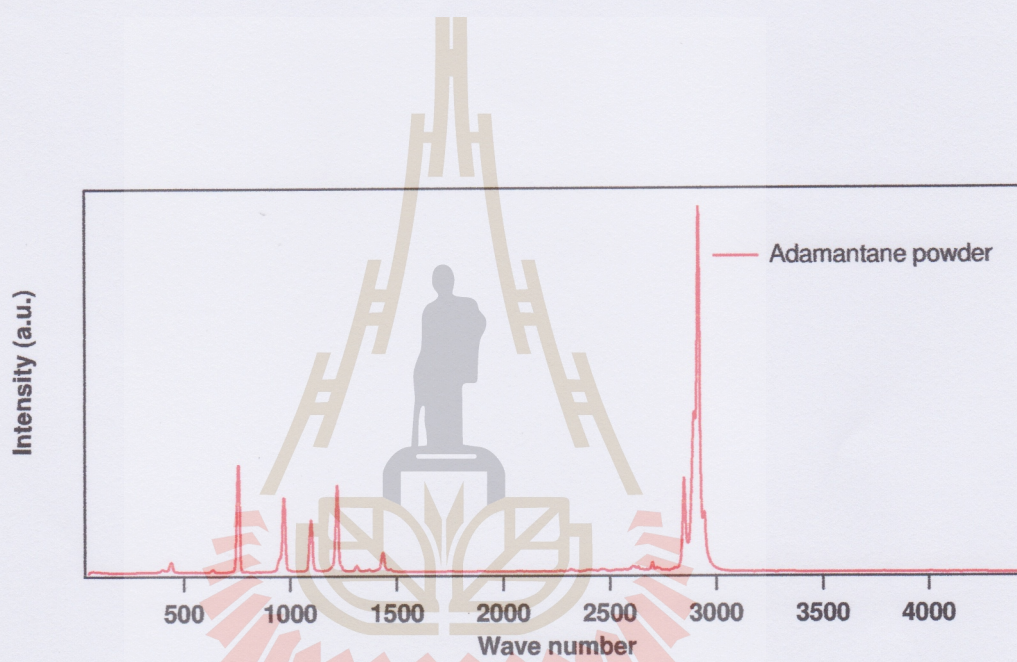
Figure 2.9 Raman spectra of adamantane powder.

CHAPTER III

FERROMAGNETISM IN CARBON-BASED

MATERIALS

In this chapter, I will describe related studies of ferromagnetism in carbon based materials. Firstly, I will introduce basic knowledges of magnetic properties, including ferromagnetism, paramagnetism, and diamagnetism. The second section contains literature reviews on the ferromagnetism and their origins studies in carbon based materials including both theoretical and experimental works. The last section in this chapter will introduce vibrating sample magnetometer.

3.1 Magnetism

The nature of magnetism has been known for over 2,500 years ago. It is physical phenomena describing the force of attraction and repulsion, occurred between electric current. A magnetic field induces particle in that field, caused by Lorentz force. The motions of electrically charged particle give rise to a magnetism. All materials act magnetism but in different interactions. They depend on the magnitude of charge, the strength of magnetic field, and intrinsic property as magnetic moment. Magnetic moment is important quantity describing magnetic properties in materials. Considering a magnet placed at an angle in external magnetic field, a torque acting on a magnet attempts to turn it into parallel the field. The moment is called magnetic moment.

3.1.1 Magnetic materials

This section will consider how magnetization can be measured. Magnetic field can be defined by two parameters as magnetic flux density (B) and field strength (H). In vacuum, the magnetic induction (B) is proportional to H-field as written in equation 3.1: note that μ_0 stands for the vacuum permeability which equals to $4\pi \ \text{x}10^{-7} \ N \cdot A^{-2}$

$$B = \mu_0 H \tag{3.1}$$

In matter, the observed induction (B) is not equal to μ_0H as measured in vacuum. Considering material placed in applied magnetic field, its magnetic moment will rearrange and then magnetize. The intensity of magnetization is M. Therefore the net induction (B) can be written in Gaussian unit and SI unit as shown in equation 3.2 and 3.3, respectively.

$$B = H + 4\pi M \tag{3.2}$$

$$B = \mu_0(H + M) \tag{3.3}$$

The magnitude of magnetization (M) can tell magnetic behavior of material. They can be mainly divided into three groups, consisting of diamagnetism, paramagnetism, and ferromagnetism.

3.1.2 Diamagnetism

Diamagnetism is a mechanism of material that repels external magnetic field; the magnetic induction field created by sample is opposite direction to applied magnetic field. The magnetization of diamagnetic material is negative and its magnetic permeability is less than μ_0. Figure 3.1 displays the magnetization process of diamagnetism. In normal state, each magnetic domain points randomly as no net magnetization. When magnetic field was applied, domain resists the ap-

plied field and orders in opposite trend to applied field. Diamagnetism is usually found in almost materials, such as carbon, silicon, quartz and water.
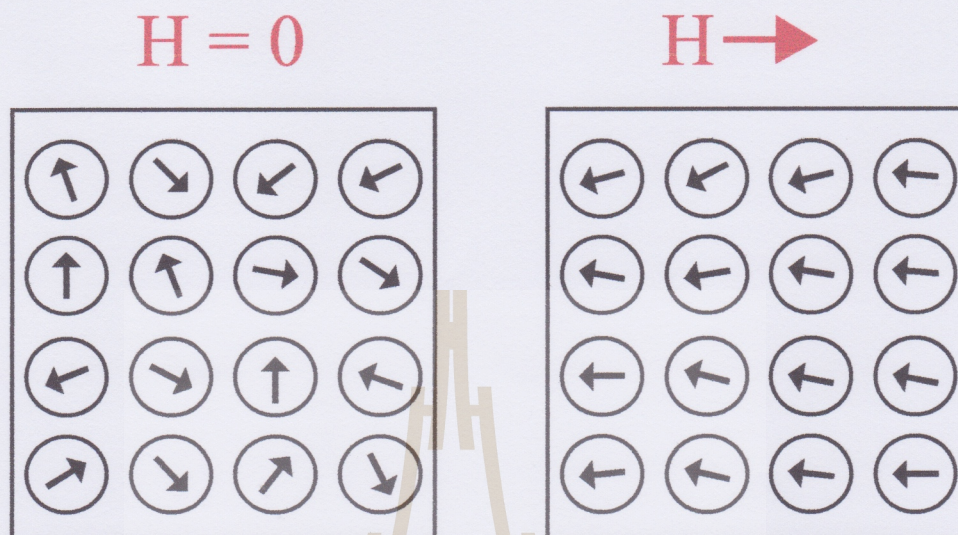
Figure 3.1 A simple schematic of diamagnetism. When external magnetic field (H) was applied in the sample, magnetic domains in each atoms will align antiparallel to the applied field.

3.1.3 Paramagnetism

Unlike diamagnetism, paramagnetism exhibits magnetic behavior that is weakly attracted to permanent magnet; the induced magnetic field is parallel to applied field. But its magnetization is very weak and cannot exist if the applied field is missing. The process of paramagnetism is presented in Figure 3.2. When the external filed was applied, domain will easily parallel to the applied field.

3.1.4 Ferromagnetism

Ferromagnetism is physical mechanism of material that can be attracted by permanent magnet. In physical view, the magnetization of ferromagnetic material
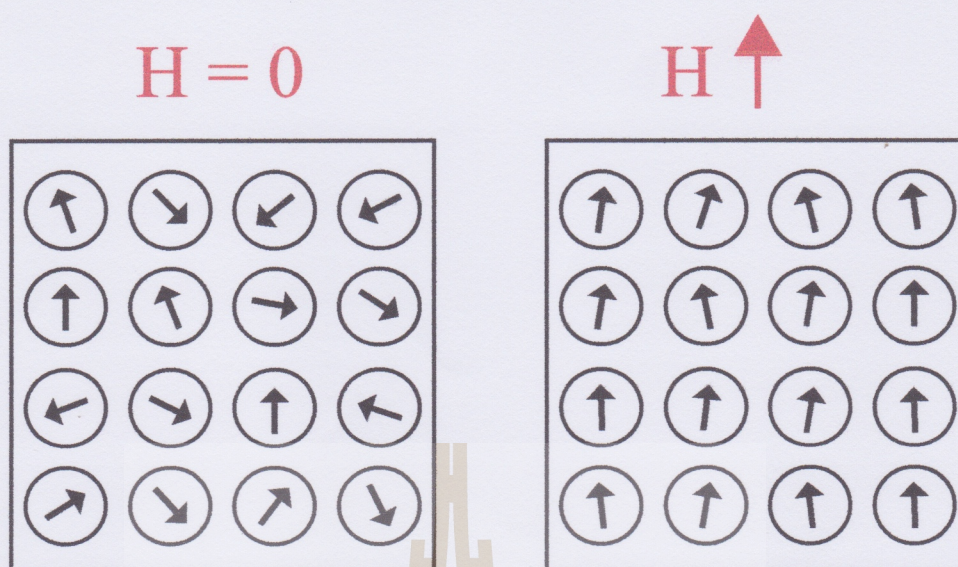
Figure 3.2 A simple schematic of paramagnetism. When external magnetic field (H) was applied in the sample, magnetic domains in each atoms will align parallel to the applied field.

is very large because its magnetic domain can still magnetize even in an absence of external magnetic field. In other words, ferromagnetic material is spontaneously magnetized. Ferromagnetism originates from unpaired electron, normally contained in d- and f-electron orbitals, to align in the parallel direction with each other domains inside material. Iron, nickel, and cobalt are most common example of this material group. Ferromagnetic materials have played an important role in modern technology, such as motor, transformer and magnetic coating in electronic devices. Furthermore, they can be used as transporter in drug delivery.

3.2 Ferromagnetic carbon materials

3.2.1 The studies of ferromagnetism in carbon based materials

Ferromagnetic behavior in carbon-based materials was first found in polymerized fullerene in 2001 (Makarova et al., 2001). Under high pressure and high temperature process, they found ferromagnetic state; saturation magnetization and attachment to a magnet at room temperature. In 2002, it was found that disordered graphite can be ferromagnetic (Esquinazi et al., 2002). This discovery was unexpected because graphite normally is strong diamagnetism. One year later, Esquinazi et. al. reported a finding ferromagnetism in proton-irradiated highly oriented pyrolytic graphite (HOPG) whose a saturation moment around 3×10^{-6} emu, please see in Figure 3.3 (Esquinazi et al., 2003). With this report, it has been found that scientists are interested in creation of ferromagnetism in metals-free materials, especially in carbon-based materials (Han et al., 2003; Wang et al., 2009; Ohldag et al., 2010; Zanolli and Charlier, 2010; Saito et al., 2011). In theoretical studies, it was reported that fullerene (C_{60}) can also become ferromagnetic (Kim et al., 2003). Similar to graphite and C_{60}, ferromagnetism was also found in other carbon types, including nano-sized diamond (Talapatra et al., 2005), Q-carbon (a new type of carbon (Talapatra et al., 2005)), Teflon (Ma et al., 2012) and Parafilm (Sriplai et al., 2015) which ferromagnetism in Teflon and Parafilm can be generated by simple method as cutting, stretching, or annealing.
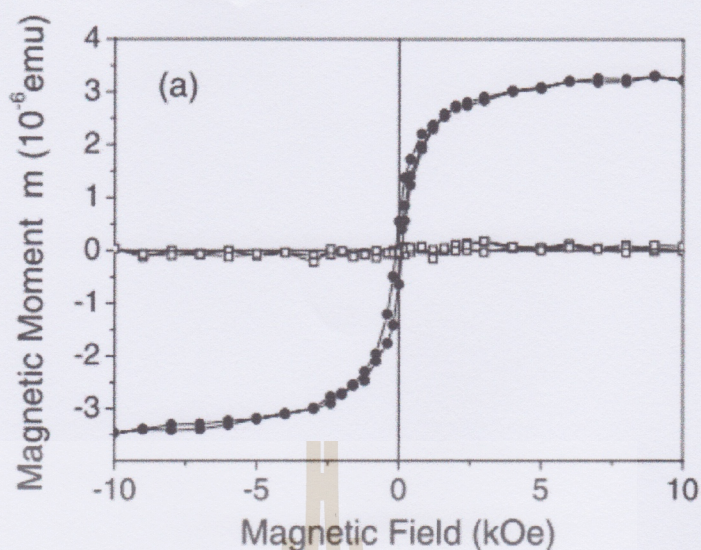
Figure 3.3 Magnetization curves of highly oriented pyrolytic graphite (HOPG) sample before (white rectangle) and after (black circle) proton irradiation. Unlike diamagnetism from the raw-HOPG, ferromagnetic signal was observed in proton-irradiated HOPG. (Esquinazi et al., 2003).
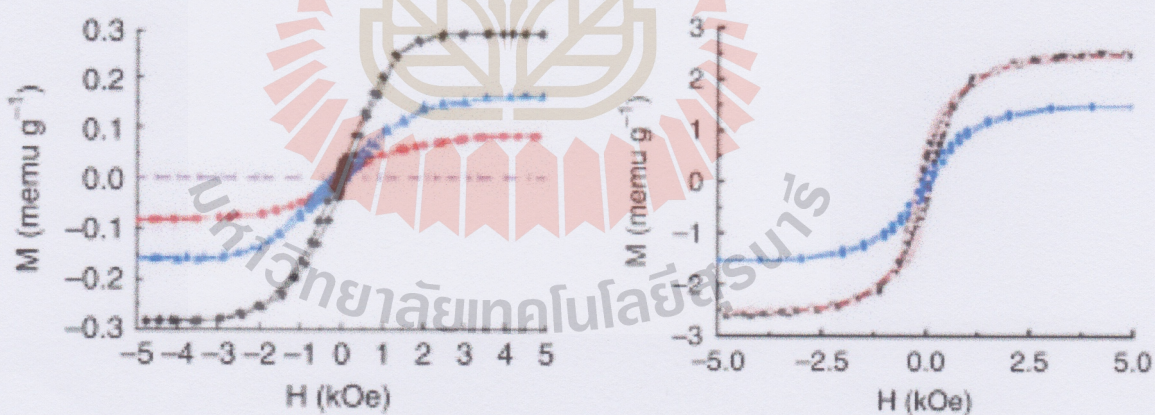
Figure 3.4 Magnetization curves of Teflon samples. By using methods, including (left) stretching and (right) annealing, Ferromagnetic behavior was observed which is the highest saturation magnetization around 2.5 emu/g (Ma et al., 2012).

3.2.2 The studies of origin in ferromagnetic carbon materials

Although many studies reported ferromagnetism in carbon based materi-

Since the conventional ferromagnetic material are mostly contained with partially filled electron in d- and f-orbital, ferromagnetism in carbons which consists of only s- and p-electron is quite strange. Scientists have tried to answer that origin of unconventional ferromagnetism. As proposed in experimental and theoretical studies, the origin mostly could come from structural defects, including carbon vacancies (Andriotis et al., 2003; Yazyev and Helm, 2007; Yang et al., 2009), nitrogen vacancies (Talapatra et al., 2005; Zhang et al., 2007), hydrogenated defect, localized π-electron and dangling bonds (Kim et al., 2003; Lehtinen et al., 2004).

One of the first discovery of carbon magnetism was found in proton irradiated graphite (Esquinazi et al., 2003). Although they did not investigate the structural carbon, they discussed it may be caused by the transformations of sp^2 to sp^3, after the proton bombardment. With this, carbon vacancy is one of proposed studies. In 2003, Andriotis et al., reported the theoretical study of carbon vacancies causing ferromagnetism in C_{60} polymers (Andriotis et al., 2003). They calculated accumulated charge between sp^3 bonds and carbon bonds surrounding vacancy. Figure 3.5 displayed the surrounding vacancy atom and sp^3 bond being at intermolecular linkage as shown in red and blue, respectively. The results of excess charge in free-vacancy sp^3 bonds was negative, whereas after the creation of vacancy, the surrounded atom gave an accumulation of excess negative charge. Electric dipole moment between those 2 positions was occurred, leading a non-zero magnetic moment.
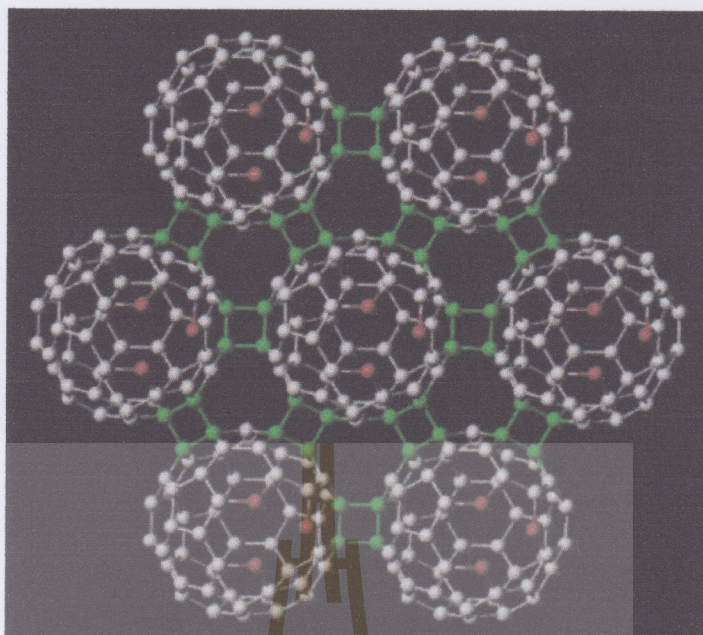
Figure 3.5 Carbon cavancies in two-dimensional rhombrohedral fullerence (C_{60}) polymers. The calculated accumulated-charge between (red) carbon vacancies and (green) intermolecular sp^3 bonds exhibits a non-zero of the total magnetic moment, suggesting the cause of ferromagnetism in this C_{60} (Andriotis et al., 2003).

In 2007 Yazyev et al., calculated ferromagnetism in graphene sheet (Yazyev and Helm, 2007). They found net magnetic spin state of graphene sheet is not zero after making vacancy; the different states of sp^2 and p_z-electron were found after the production of defect, please see in Figure 3.6.

Since the early studies of ferromagnetism in carbon based material was using proton irradiation which possibly causes structural defects, other elements also were also uses as irradiation sources. In 2005, Talapatra et al., used nitrogen (^{15}N) and carbon (^{12}C) ion for implanting in carbon nano strutures (Talapatra et al., 2005). They found nitrogen ion irradiation produces higher magentization than carbon irradiation, compared to the carbon irradiation in the same doses, as shown in Figure 3.7. The significant amount of ^{15}N trapped in graphitic structure, observed by a presence of XPS, was believed to be a origin of that ferromagnetism.
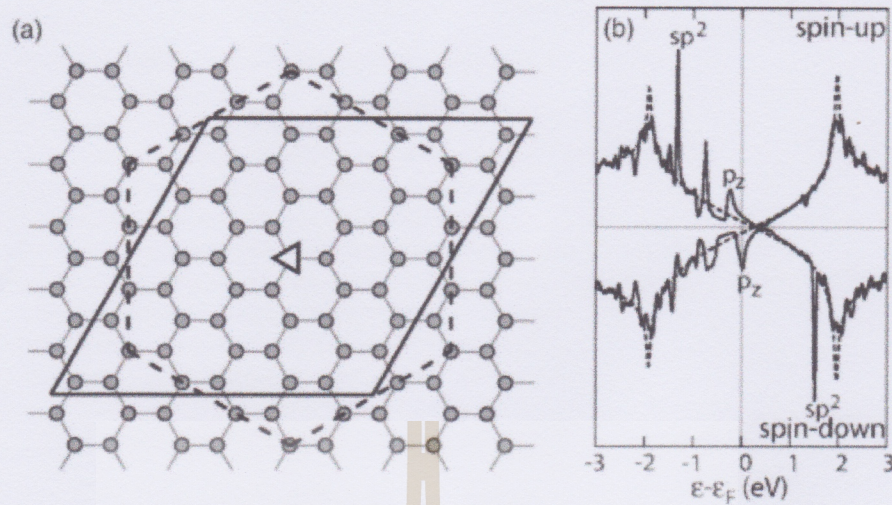
Figure 3.6 (a) The calculated size of hexagonal graphene sheet with the defective atom labeled by triangle at the center. (b) Density of states plot for system with the vacancy defects. The dash line is state from ideal graphene (Yazyev and Helm, 2007).

Theoretical study of nitrogen vacancy affected to ferromagnetism in carbon based material was reported later in 2007 (Zhang et al., 2007). They calculated a magnetic moment of graphite which has 2 structural vacancies. The first is from carbon vacancies and the second was divided into 2 cases, consisting the relative another carbon vacancy and nitrogen vacancy. Figure 3.8 presented the magnetic moment of nitrogen vacancies is higher than the second carbon vacancy at some positions. These suggested that nitrogen vacancy can change spin states, leading the presence of ferromagnetism.

There is another origin of ferromagnetism that researchers have been interested, called "Dangling bond". This is an unpaired electron, occurred in disordered structure and is found in carbon material. Carbon dangling bond is produced by the creation of defect, i.e. irradiation, causing the unpaired electron. Unlike π-electron that can move freely, this unpaired electron is localized at the edge of defect
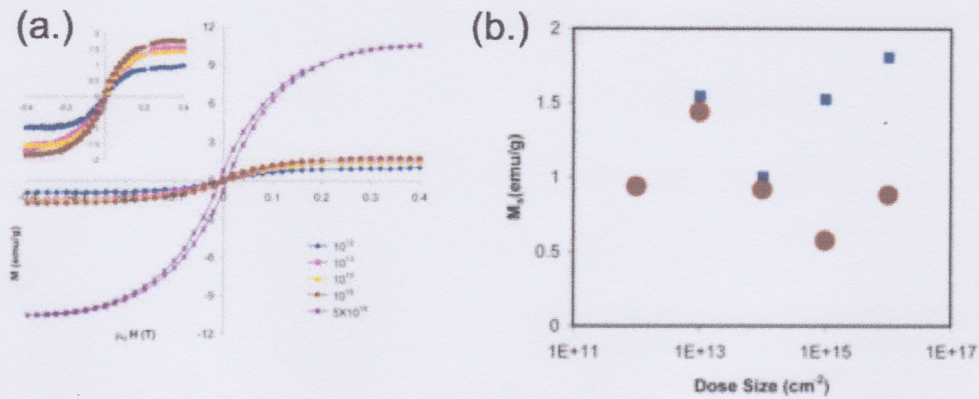
Figure 3.7 (a) Magnetization curves of nitrogen-implanted graphite from various doses. (b) The comparison of saturated magnetic moments for ^{15}N (solid squares) and ^{12}C (circles) irradiations, adapted by (Talapatra et al., 2005).

Nitrogen adatom position	Magnetic moment (μ_B)	2nd vacancy	Magnetic moment (μ_B)
X_a	3.00	X_a	0.00
X_b	1.00	X_b	2.00
X_c	1.00	X_c	2.00
X_d	3.00	X_d	0.00
X_e	3.00	X_e	0.00
X_f	3.00	X_f	0.00
X_g	1.00	X_g	2.00
X_h	3.00	X_h	0.00
X_i	1.00	X_i	0.00
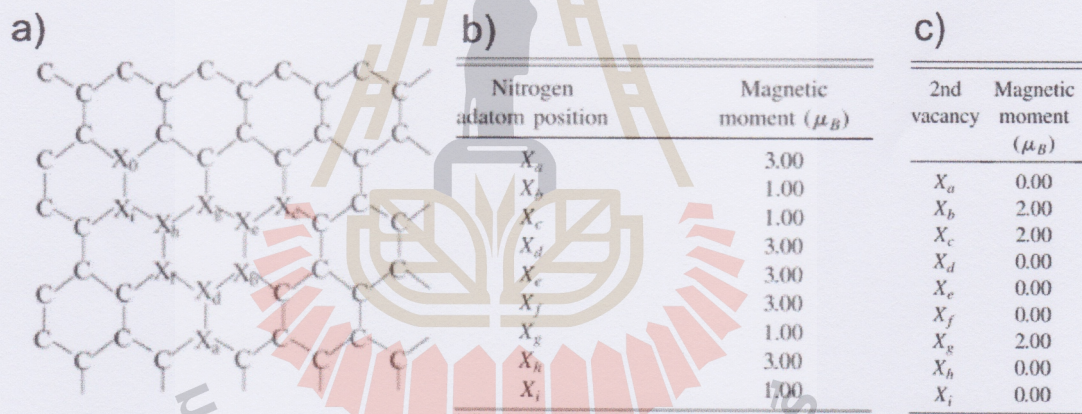
Figure 3.8 (a) The model configuration of graphite structure including of two vacancies. X_0 indicated the position of first vacancy, and X_{a-i} indicated the relative position of the second vacancy. In case of nitrogen irradiation, X_{a-i} indicated the relative position of nitrogen atom. (b) The position of second vacancy and magnetic moments of graphite. (c) The position of second vacancy and magnetic moments of nitrogen datom, adapted by (Zhang et al., 2007).

position. Figure 3.9 displayed an example of dangling bond; when a carbon atom was removed from graphene, 3 sp^2- dangling bonds surrounded the removed one

were produced. Dangling bond in fullerene was theoretically studied in 2003 (Kim et al., 2003), after the experimental work in 2001 (Makarova et al., 2001). Kim et al., calculated spin-density of various opened-cage fullerenes. Non-zero magnetic moments of disordered fullerenes were found at zigzag structures, as shown in color atoms at Figure 3.10 a. They also proposed that not all models of dangling bonds produce ferromagnetism. If the localized electrons align in opposite way, the magnetic moment will be canceled out. The Figure 3.10.b showed the comparison of ferromagnetic and antiferromagnetic models of disordered fullerene.
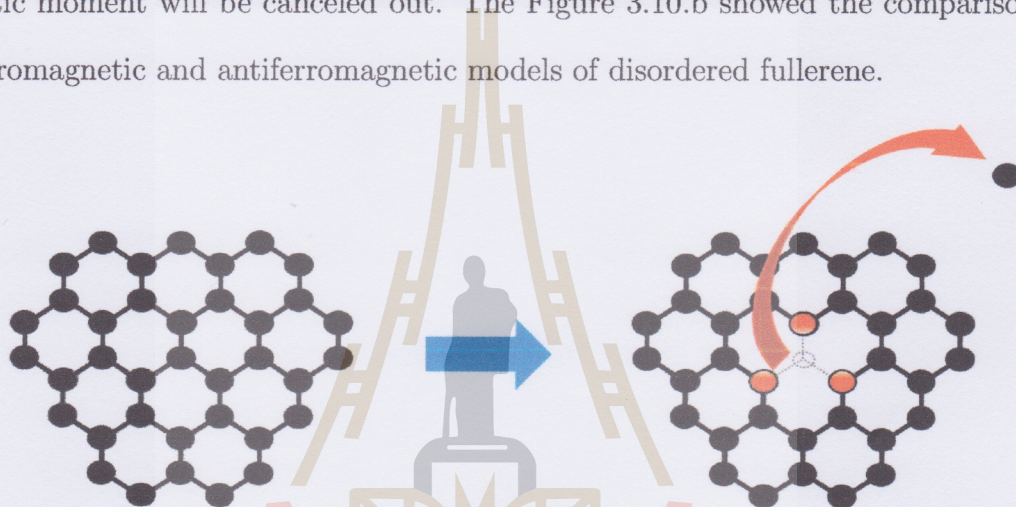
Figure 3.9 Simple schematic diagram of (a) graphene and (b) the 3 dangling bonds that are removed from its structure.
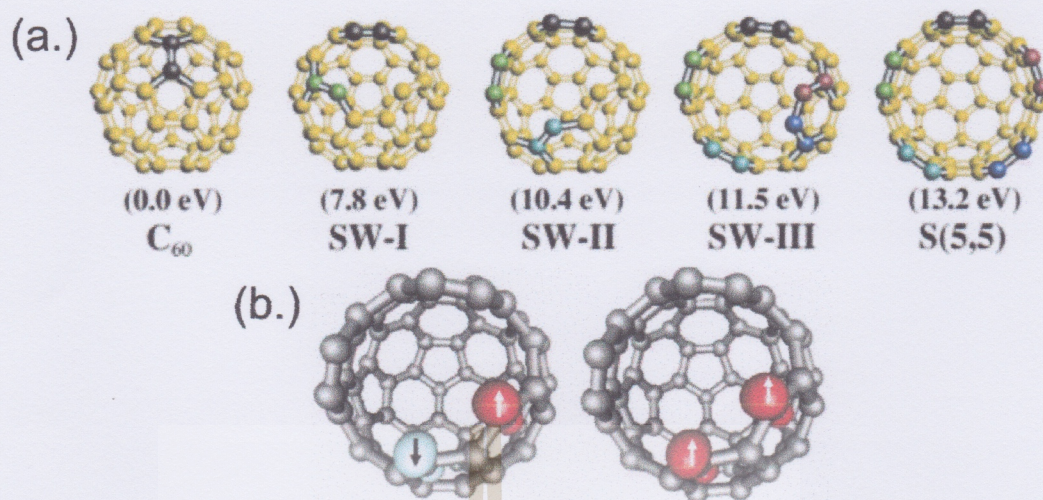
Figure 3.10 (a) Models of intermediate structures during the transformation of C_{60}. Carbon atoms surrounding the missing atoms are indicated by different colors. (b) Spin-density surfaces for ferromagnetic and antiferromagentic models. Red atom (white-blue) surfaces represent density of spin-up (spin-down) electrons (Kim et al., 2003).

Dangling bond is also theoretically studied in graphite (Lehtinen et al., 2004). With removing a carbon atom, each of three neighboring atoms has a sp^2 dangling bond. Two of these dangling bond formed covalently together, leaving a dangling bond. This localized electrons contribute to the observed magnetic moment. Reconstructed carbon nanotubes (CNTs) were observed in six years later (Zanolli and Charlier, 2010). The mono-, di- and tri-vacancies of reconstructed CNTs displayed the dangling bonds and new carbon bond, after the creation of defects, as presented in Figure 3.11.
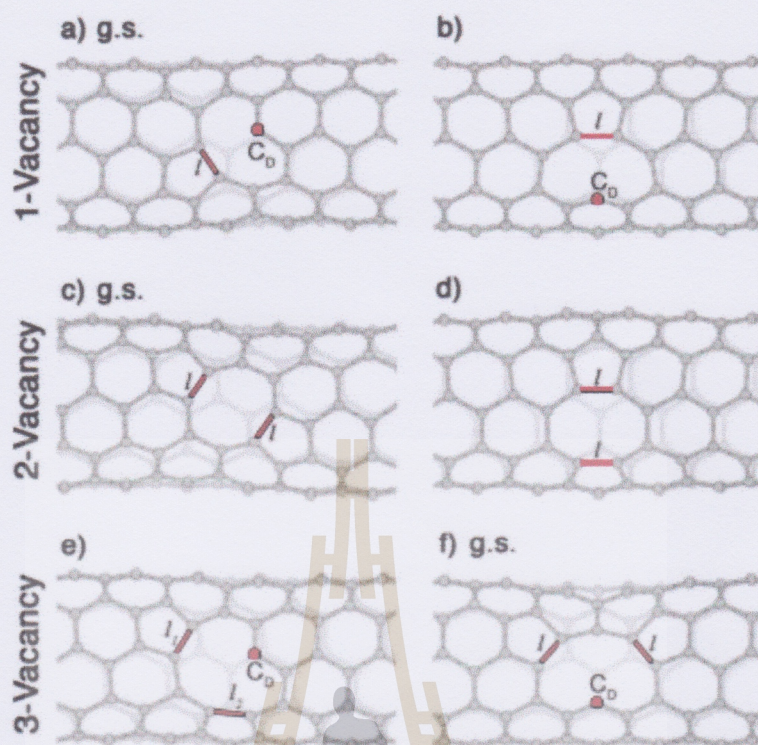
Figure 3.11 The model of carbon nanotubes containing a reconstructed vacancies (a, b), di-vacancies (c, d) and tri-vacancies (e, f). The most stable states for each vacancies are represented as ground state (g.s). The newly carbon form and dangling bond are indicated by 1 and C_D (Zanolli and Charlier, 2010).

Recently, it was found that dangling bond can be created in metal-free polymer as Teflon (Ma et al., 2012). As proposed in calculation part in this work, dangling bonds were created by cutting, heating, or stretching method, leading to be ferromagnetic in Teflon. Note that Figure 3.12 displayed the schematic illustrations of these methods and the dangling bond occurred at edge of disordered areas.
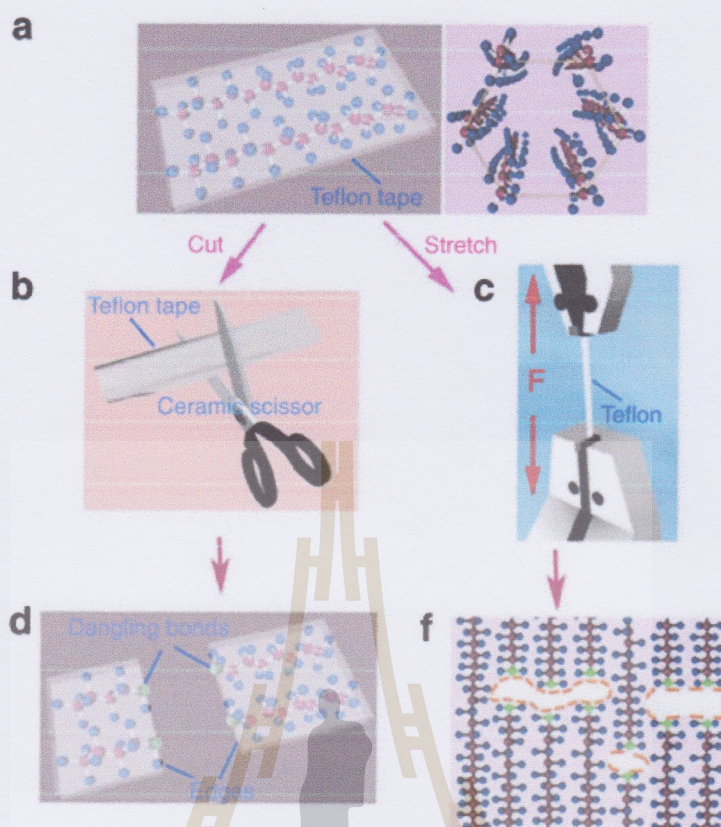
Figure 3.12 (a) Schematic illustrations of carbon compound in Teflon. (b) Model of (b) cutting and (c) stretching of Teflon tape. (d, f) Model of dangling bonds created after cutting and strentching (Ma et al., 2012).

In 2010, Ohldag et al., reported the first direct evidence of microscopic origin of ferromagnetism in irradiated graphite (Ohldag et al., 2010). By using x-ray magnetic circular dichroism (XMCD), they found magnetic moment of polarized π-electron which caused ferromagnetism as shown in Figure 3.13. Furthermore, they found hydrogenated π-state can also produce ferromagnetism. This work confirmed that ferromagnetism can be produced in carbon based materials.
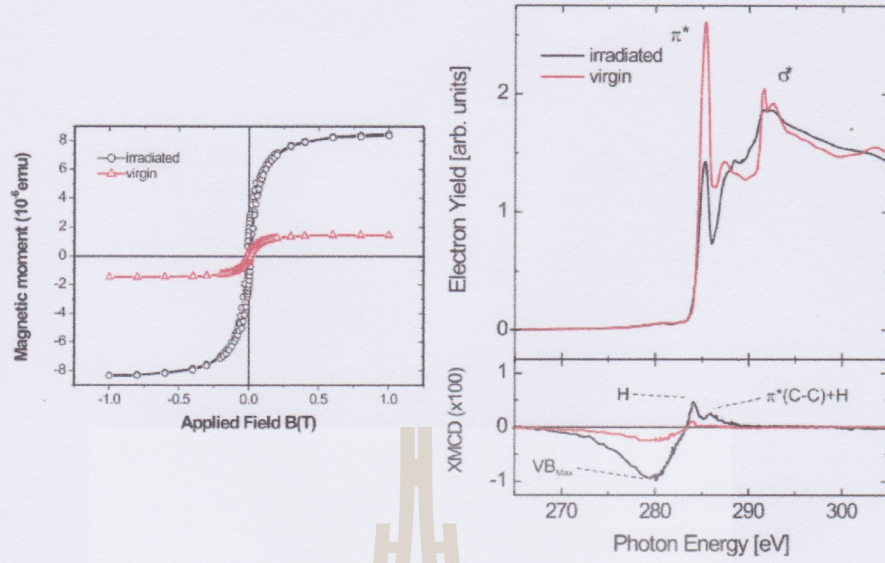
Figure 3.13 (left) Hysteresis loop measured by SQUIDt 300K for the irradiated (black) and the virgin (red) graphite samples. (right) X-ray spectrum and XMCD difference of the irradiated (black) and the virgin (red) graphite samples. (Ohldag et al., 2010).

3.3 Vibrating Sample Magnetometer

Vibrating sample magnetometer (VSM) is a technique used to study magnetism by measuring flux changes from magnetized sample. It was first introduced by Simon Foner who worked at Lincoln laboratory, Massachusetts Institute of Technology in 1959. This technique is based on Faraday's law which states that the change of magnetic flux (σ) can induce electromotive force, as displayed in equation 3.4.

$$\epsilon = -\frac{d\sigma}{dt} \tag{3.4}$$

In VSM measurement, sample usually is powder or film. The sample, attached on non-ferromagnetic holder, was placed inside measured tube, connected to pickup coils and electromagnets which is used to generate uniform magnetic field. Sample

was vibrated along vertical direction and detector can detected flux changes as presented in Figure 3.14. VSM is very sensitive; it can be used for measuring of
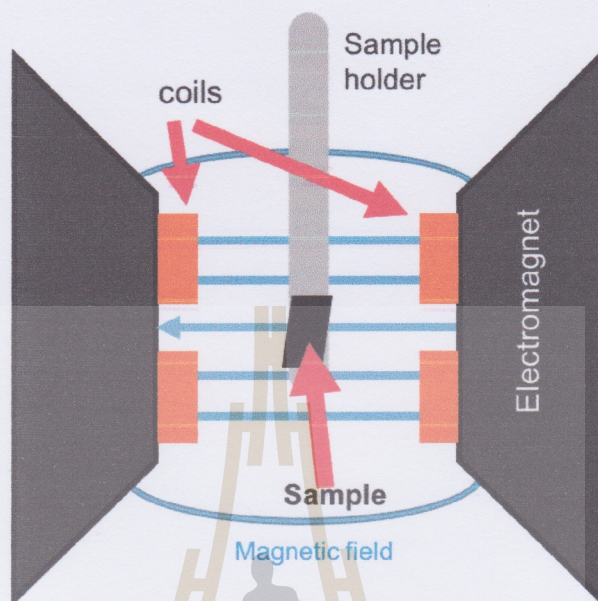
Figure 3.14 The model of vibrating sample magnetometer (VSM) measurement

both strongly and weakly magnetizations. Typically, VSM can detect magnetic moment as less than 10^{-5} emu. Furthermore, magnetic measurement as a function of temperature can be observed by using VSM. It can decrease temperature as less than 50K and heat higher than room-temperature (300K).

3.3.1 Hysteresis loop

One of the best way to obtain information about magnetic properties of material is studying hysteresis loop. A hysteresis loop carries the relationship of magnetization of sample (M) and the applied field (H), or called magnetization curve or M-H curve. The hysteresis loop example of ferromagnetic material is shown in Figure 3.15. This loop is created by measuring the induced flux of ferromagnetic material, magnetized by external field. Considering ferromagnetic sample placed in applied magnetic field, when applied field was gradually increased, the
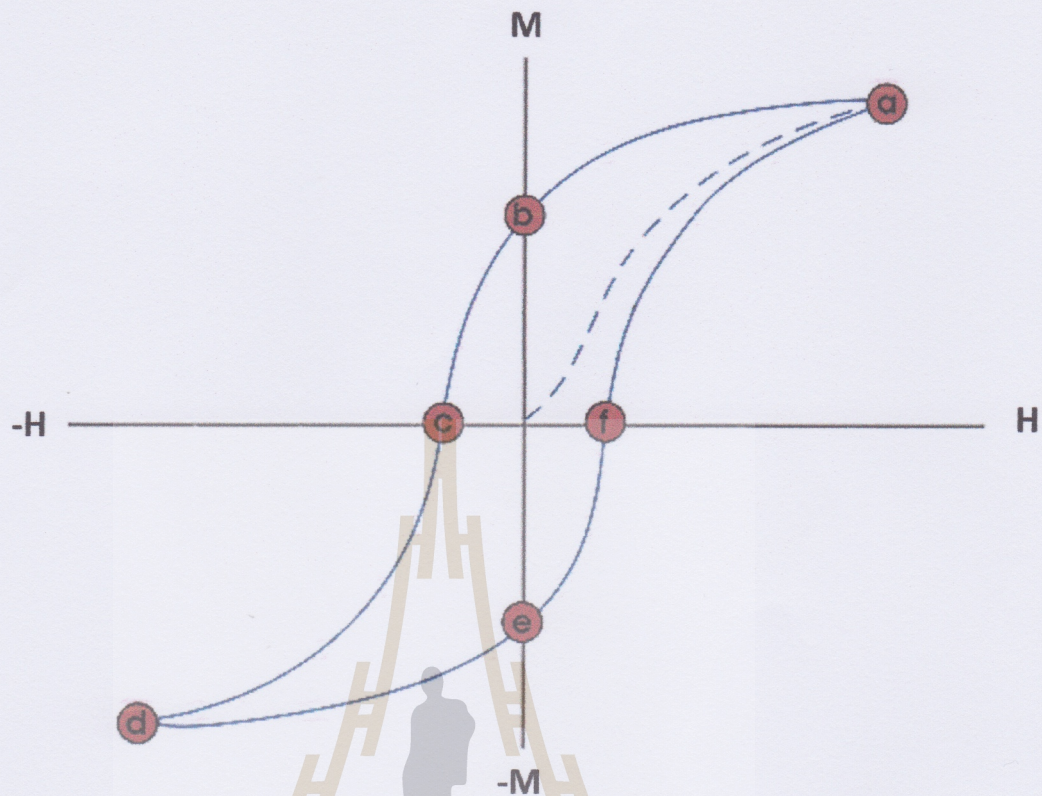
Figure 3.15 Hysteresis loop model of ferromagnetic material. First, when magnetic field was applied, magnetization will increase gradually until it saturates. After that, the magnetization is gradually reduced from the saturation to zero, when the magnetic filed was applied in opposite direction, leading to hysteresis loop.

magnetization will increase caused by the alignment of magnetic domain parallel to the field, presented by dash line in Figure 3.15. At point (a), almost of magnetic domain are aligned in field's direction; the magnetization will never increase, or increase a little bit, even we applied higher magnetic field. This point is called saturated magnetization (M_s). When the applied field was reduced to zero, magnetic domain was demagnetized and the magnetization curve will move down to position (b). Point (b) presents the remaining magnetization of ferromagnetic sample

that can saturate itself even the absence of applied field. This mechanism is called remanent magnetization or retentivity. Since the applied field was reversed, curve moves to point (c) which is called coercivity field (H_c). This value can tell the amount of applied field which must be applied to totally remove magnetization in material. As applied field was increased negatively, magnetic domain will magnetize and saturate again, but in opposite direction. The curve will go to point (d). Like reducing positive applied field, the curve will reduced to point (e) and (f) when the applied field was reduce to zero and increase it again, respectively.

CHAPTER IV

ORIGIN STUDY AND ENHANCEMENT OF FERROMAGNETISM IN CVD-CARBON FILMS

Ferromagnetism is observed in carbon-film prepared by using adamantane as precursor. We use chemical vapor deposition (CVD) technique for creating carbon film because we believe this CVD technique provide some structural defects (which is the cause of ferromagnetism in Teflon and Polymers (Ma et al., 2012; Sriplai et al., 2015)), leading to occur ferromagnetism in CVD-carbon films. The physical properties of the CVD-carbon films including film thickness, measured by using scanning electron microscopy, will be showed in section 4.1. In section 4.2, the discovery of unconventional ferromagnetism that does not occur by magnetic element (such as Fe, Ni, and Co) in our CVD-carbon films will be presented. To confirm that there are no any metal elements contaminated, the chemical composition characterization, measured by using energy dispersive x-ray spectroscopy and x-ray photoemission spectroscopy, will be presented in section 4.3.1 and section 4.3.2, respectively. This suggests an inexpensive CVD technique is a new way to create magnetic materials. Intriguingly, this ferromagnetism could be further enhanced when our carbon films are excited by high intensity laser and saturated magnetization could be highly strong enhanced when the films are mechanically exfoliated. This phenomenon will be revealed in section 4.4. To understand the origin of ferromagnetism in CVD-carbon films, we used Raman spectroscopy to characterize various types of carbon bonding in the sample, including sp^2, sp^3,

C-H bond and especially defect bonds which may be the cause of ferromagnetism in our films, similarly the cause in Teflon (Ma et al., 2012).

4.1 CVD-carbon films prepared by using adamantane as precursor

Regarding to the film preparation, we used adamantane powder with purity of 99.0 % (Acros Organics, Belgium) as the precursor material. The films were prepared on substrates, including quartz (SiO_2), sapphire, silicon, sand and also rice husks. Note that the film preparations were operated in high vacuum atmosphere in order to protect any undesirable reactions. Figure 4.1 illustrates the particularly physical character of the CVD-carbon films. The topography and thickness of the films was observed by using scanning electron microscopy(SEM). Figure 4.1(a) and 4.1(b) demonstrate a pure quartz substrate before and after carbon film using adamantane as precursor was deposited. In contrast with pure quartz which is colorless, the CVD-carbon film has a black color but it is still be transparent as the letter "S" underneath the film can be appeared. The morphology of the quartz substrate and CVD-carbon film was also observed. As shown in Figure 4.1(d), patches with a few microns in length scale along the plane were observed in the CVD-carbon films, conflicting to the substrate before the deposition(Figure 4.1(c)). The thickness of the films was measured from the cross section technique. Figure 4.1(e) exhibits an average thickness of 1.43 μm for the CVD-carbon film which we used to evaluate actual ferromagnetism ($emu \cdot g^{-1}$) of our CVD-carbon films. Figure 4.1(f) shows the picture of non-magnetic sand grains covered with thin CVD-carbon films which could stick to an strong neodymium magnet.
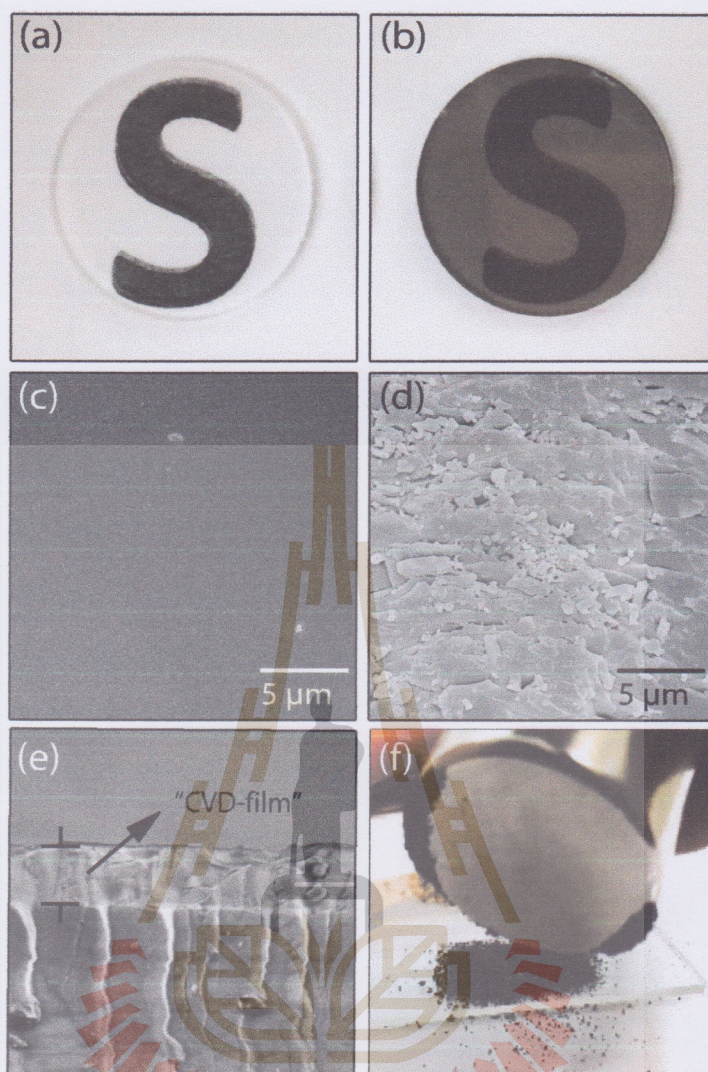
Figure 4.1 The observation of (a) pure quartz (SiO_2) and (b) CVD-carbon film, prepared by using adamantane as precursor. This carbon film is black but still be transparent. Topology of 18x18 μm^2 SEM-images (with 10K magnification) of (c) a heated pure quartz and (d) the CVD-film on quartz substrate were observed. (e) Cross section SEM-image reveals CVD-film layers on top of quartz substrate with its thickness around 1.429μm. Picture of (f) sand with coated CVD-carbon film attracting to a permanent magnet.

4.2 Ferromagnetism in CVD-carbon films

All the magnetic properties measurements were conducted by using vibrating sample magnetometer (VSM) at Khon Kean University (KKU). We applied

external magnetic fields under from -15,000 Oe to 15,000 Oe under wide range of temperature between 50 K to 390 K. At room temperature observation, the observed ferromagnetic behavior mixed together with the diamagnetic signal of our sample, including pure diamagnetic behavior from a heated quartz substrate are shown in the upper-left inset of Figure 4.2, presented by red and black line, respectively. The main graph in Figure 4.2 presents room-temperature ferromagnetism in the as-grown carbon with the saturated magnetization of around 6.2 $emu \cdot cm^{-3}$;note that the presented data was already subtracted by the diamagnetic signal of the quartz substrate. While the another inset displays a magnification of hysteresis loop at near zero applied magnetic field. It is easy to see that coercivity is approximately 40 Oe. To study temperature dependence of the magnetic property in our CVD-carbon film, Figure 4.3(a) shows the M-H curves of CVD-film measured at various temperature between 50 K and 390 K. The saturation magnetization of the CVD-carbon film prepared by using adamantane as precursor gradually increased as temperature decreased. The temperature dependence of magnetization of this sample shows characteristic of typical ferromagnetic materials, as shown in Figure 4.3(b). It was found that ferromagnetic signal exhibited a large saturation magnetization of 7.9 $emu \cdot cm^{-3}$ at 50 K.
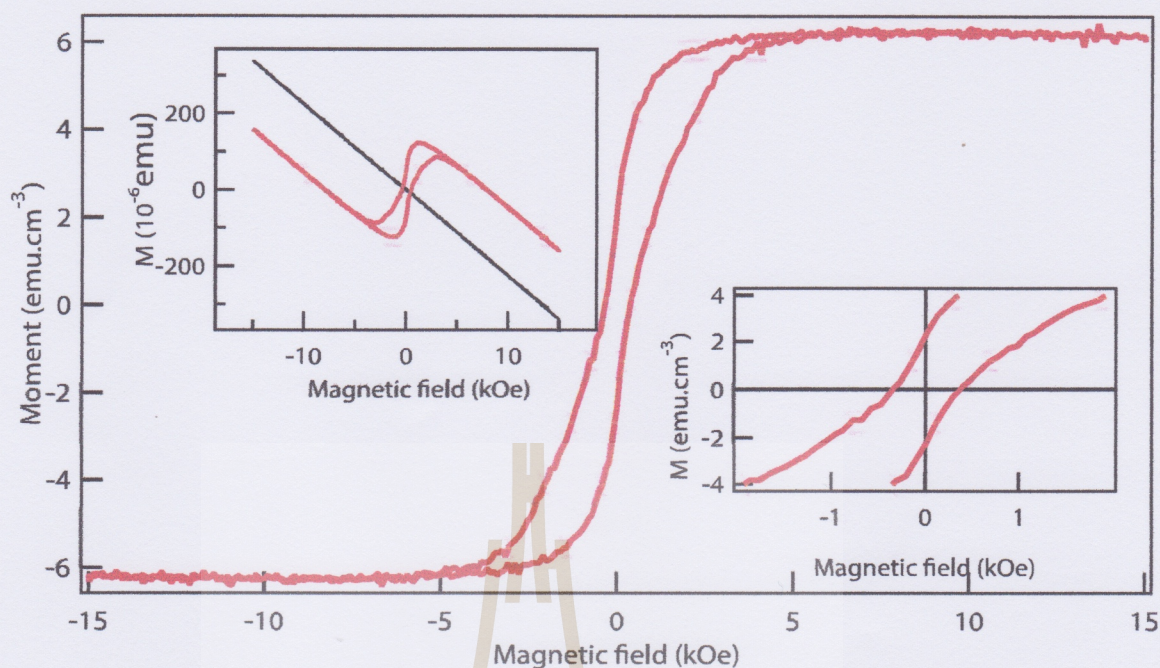
Figure 4.2 M-H curve, subtracted by diamagnetic background, of the carbon film shows ferromagnetic signal with high saturation as $6.2\ emu \cdot cm^{-3}$. Top inset shows (red) ferromagnetic signal, before background subtraction, of CVD-film and (black) diamagnetic signal of a heated quartz, while the bottom inset reveals a magnification of hysteresis loop.

4.3   Chemical Characterization of CVD-carbon film

Since the saturated magnetization of CVD-carbon film prepared by using adamantane as precursor was moderately strong, it is important to examine impurities the effect of metal impurities, such as Fe, Co, or Ni, in our CVD films. In this section, therefore I will present chemical analysis of the CVD-carbon films by using energy dispersive x-ray spectroscopy (EDS), including x-ray photoemission spectroscopy (XPS).
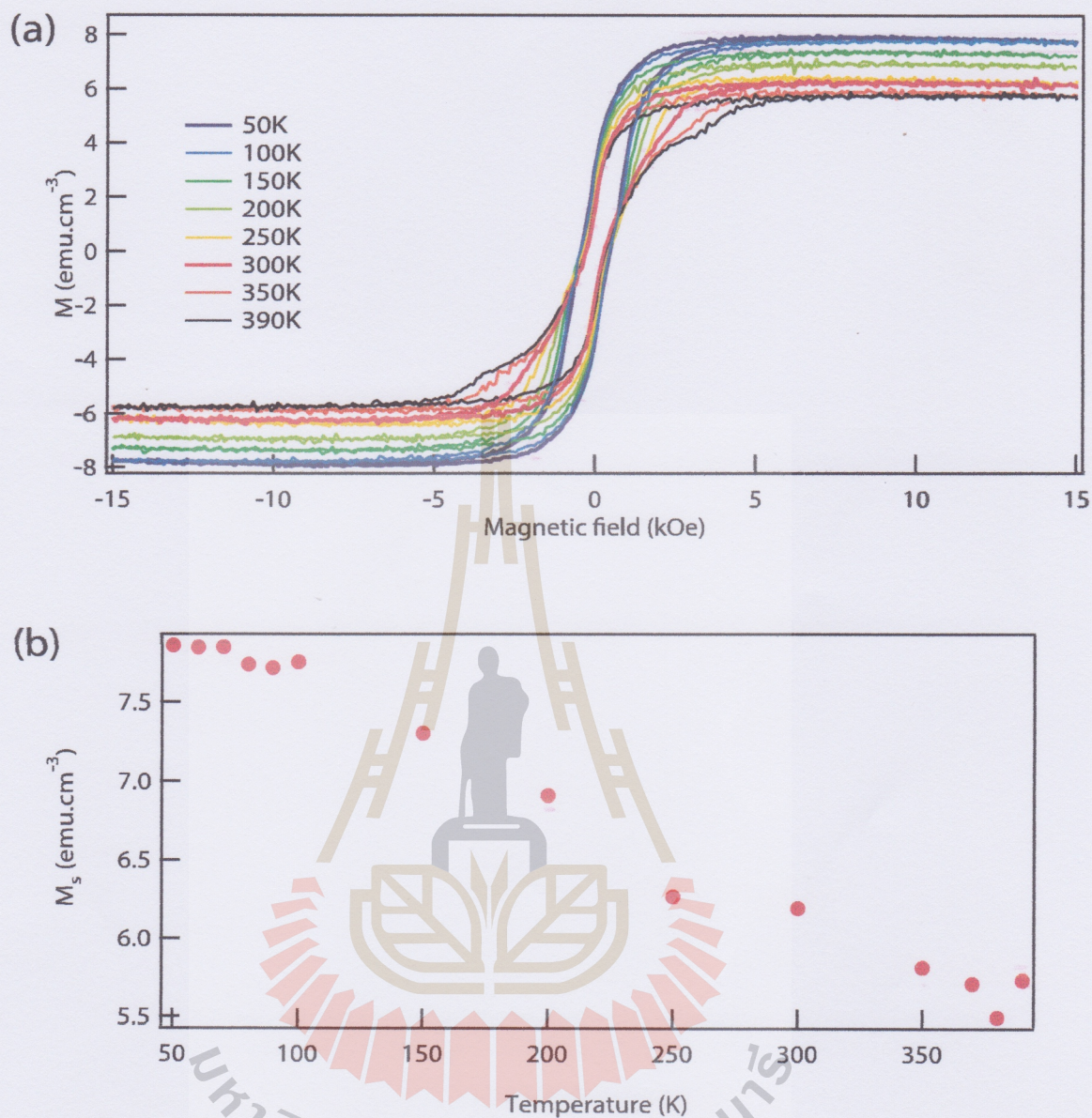
Figure 4.3 (a) M-H curves as a function of temperature from 50K to 300K of CVD-carbon film. (b) The saturation magnetizations increased after measuring at lower temperature, suggesting a characteristic of ferromagnetic material.

4.3.1 Energy dispersive x-ray spectroscopy of CVD-carbon film

Since we found strong saturated magnetization signal in CVD-carbon film prepared by using adamantane as precursor, metal contaminated characterization

is first aspect to observe. By using energy dispersive x-ray spectroscopy (EDS) with the sensitivity of 1000 ppm (or 0.1%), Figure 4.4 exhibits EDS of CVD-carbon films. In Figure 4.4 (a), without any magnetic composition such as Fe, Co, and Ni (as shown in magnification inset), we found 3 elements consisting of C, O, and Si, at substrate position, where the red star represents to measured point. Regarding the film point observation, there is only carbon found. With these data, we can safely confirm the magnetic elements (Fe, Co, and Ni) are not the origin of the ferromagnetism observed in CVD-carbon films. To emphasize this aspect, if our films contain some small amount of magnetic metals, they should be detected. For an example, if iron (Fe) impurity were the cause of the observed signal (Figure 4.4), they should have been roughly 1% Fe ($emu \cdot g^{-1}$), or more than 10 times of the senstivity of EDS that could be easily observed. Therefore, we surely confirm that ferromagnetism in CVD-carbon films does not arise from transition metals.

4.3.2 X-ray photoemission spectroscopy of CVD-carbon film

To another examine chemical composition, we used x-ray photoemission spectroscopy at Synchrotron Light Research Institute (SLRI) for measuring magnetic element impurities. Figure 4.5 shows photoelectron spectra of CVD-carbon films. With using photon energy 400 eV, we found no trace of magnetic element (e.g. iron, nickel, and cobalt) as there are no peaks at the labeled points in magnification inset.
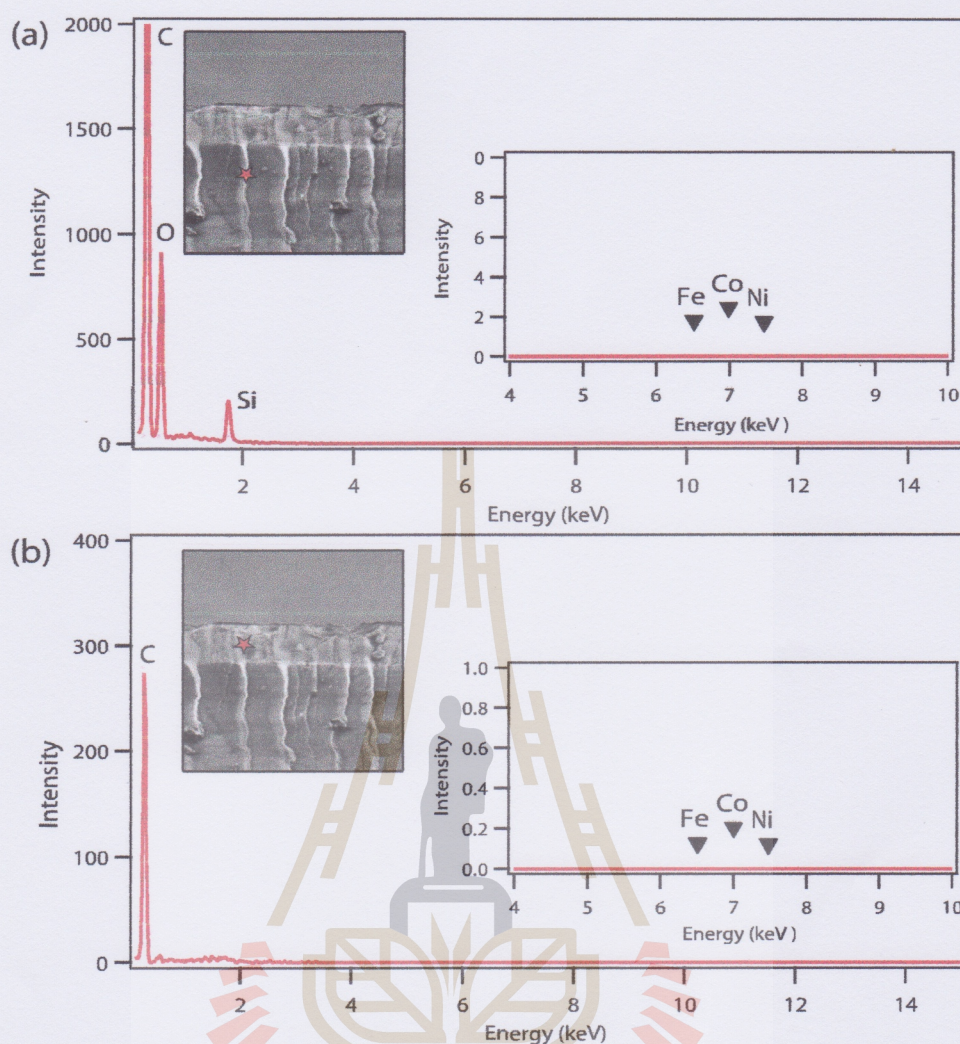
Figure 4.4 Energy dispersive x-ray spectra of the CVD-film at both (a) substrate and (b) film position, labelled by red star, show the non-existence of magnetic elements signal, including iron, nickel, and cobalt.

4.4 Origin study of ferromagnetism in CVD-carbon films

As proposed in other studies that the origin of ferromagnetism in pure carbon could be structural defects, therefore we studied chemical bonds in CVD-film by using Raman spectroscopy. As shown in Figure 4.6, the Raman spectra of CVD-carbon film reveals 3 obvious peaks at 1,331 cm^{-1}, corresponding to sp^3 bonding (called D-peak, or disorder peak), 1,574 cm^{-1}, corresponding to sp^2 bonding (called
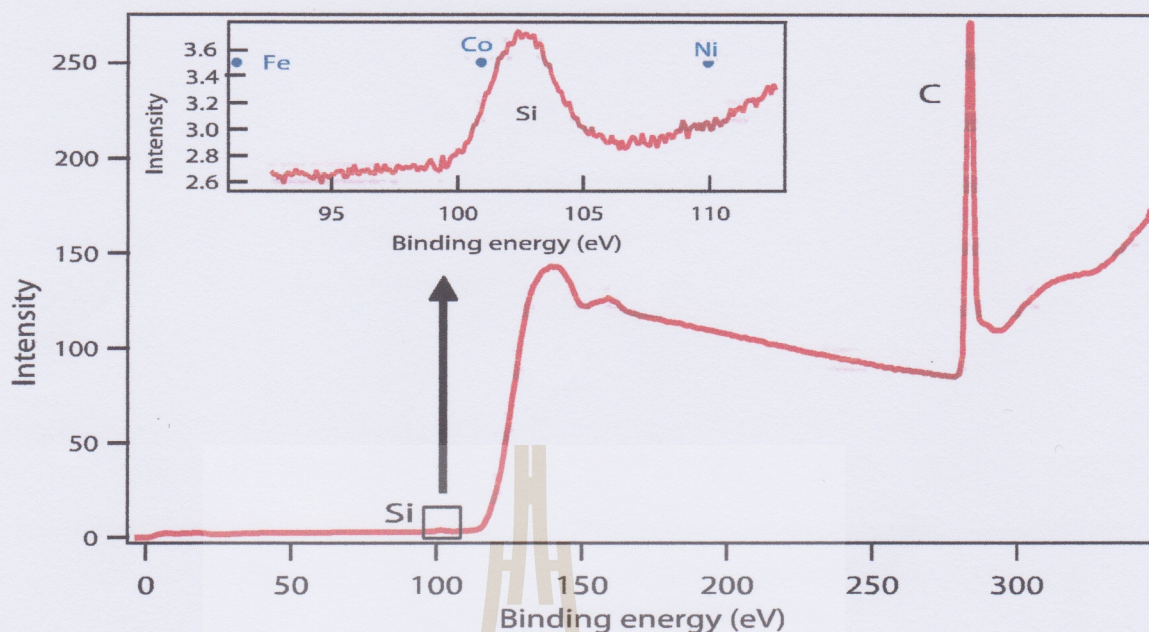
Figure 4.5 Photoelectron spectra of the CVD-carbon film, measured by using photon energy 400eV, exhibit a clear evidence that there are no any peaks of magnetic elements such as iron, nickel, and cobalt. This suggests our measured ferromagnetism do not come from magnetic metal impurities.

G-peak, or graphite peak) and 2,750 cm^{-1} which is relatively more broad, corresponding to C-H bonding. The ratio of D-peak and G-peak areas is approximately 2.4: 1. As proposed by Saito et al., (Saito et al., 2005), ferromagnetism in the DLC film was found to be stronger in a sample with larger amount of sp^3 bond. Similarly, Ma et. al. also reported his experimental study of ferromagnetism in Teflon which came from dangling bond created in stretching and heating method. Since adamantane ($C_{10}H_{16}$) is only sp^3 bonding and the ratio between C and H atoms is also high (1: 1.6), the creation of various carbon types could suggest the dangling bond. In other words, carbon-dangling bonds may be produced during CVD process and could be the main cause of ferromagnetism in our films.

Furthermore, it was found that the Raman spectra of CVD-carbon film was changed after laser irradiation. In this case, we used green laser source of 532
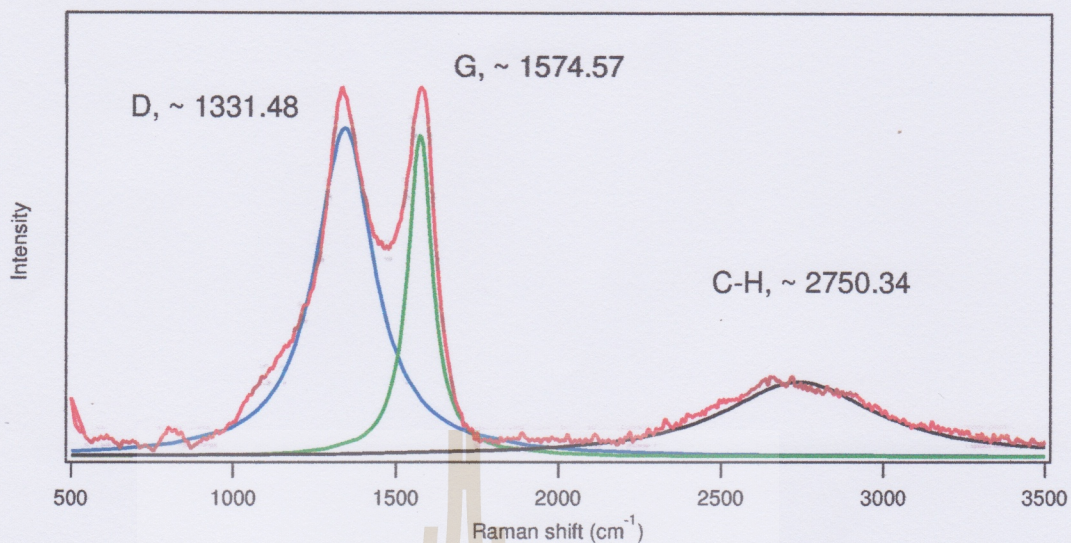
Figure 4.6 Raman spectra of CVD-film on quartz shows signals of G-peak, relating for sp^2, D-peak, relating for sp^3, and C-H bond.
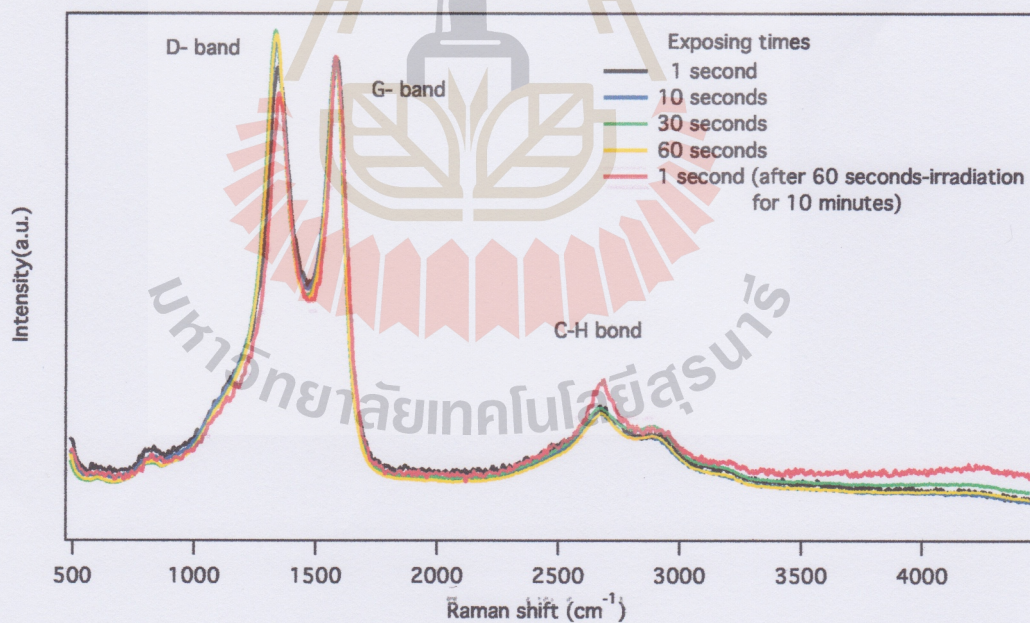
Figure 4.7 Raman spectra of CVD-film after green-laser irradiation.

nm and irradiated on various exposing times between 1 second to 60 seconds as shown in Figure 4.7. The intensity of Raman peak at 1,343 cm^{-1}, represented

for disordered peak (D-peak), is increased after increasing exposing time of laser irradiation. Note that we calculated by fixing graphite peak (G-peak). However the D-peak moves lower than the previous measurements after we closed laser and leaved the sample for 10 minutes before measuring. In addition, the C-H bond peak changes slightly in the last measurement. This suggests the laser irradiation could change the structure.

4.5 Enhancement ferromagnetism in CVD-carbon films

In 2003, Kim et al., who study ferromagnetism in fullerene, reported some dangling bond models can be ferromagnetic (Kim et al., 2003). As presented at Figure 3.10.b, if their spins point in opposite direction, dangling bond model will be antiferromagnetic. In this section, I will present the increases of ferromagnetism after mechanically exfoliation and laser irradiations.

4.5.1 Mechanically exfoliation effect

Since we produced film by using CVD technique operating under 1,050 °C, our film will be amorphous carbon deposited on substrate. Therefore dangling bond may be occurred randomly. However, due to using quartz crystal as substrate, we believe the carbon film layers near substrate may be higher orientation than the upper layer. To increase the alignment of dangling bond, I try to exfoliate upper layers of CVD-film. GE varnish glue, which is normally used to mount sample in VSM measurement, was used to exfoliate; therefore it was confirmed the glue will not be effect to the measurement. The result shows in Figure 4.8. The original ferromagnetic signal is shown as the black curve. After the exfoliation, saturated magnetization is further enhanced and goes to around 8.4 times after almost exfoliation, indicated by the red line.
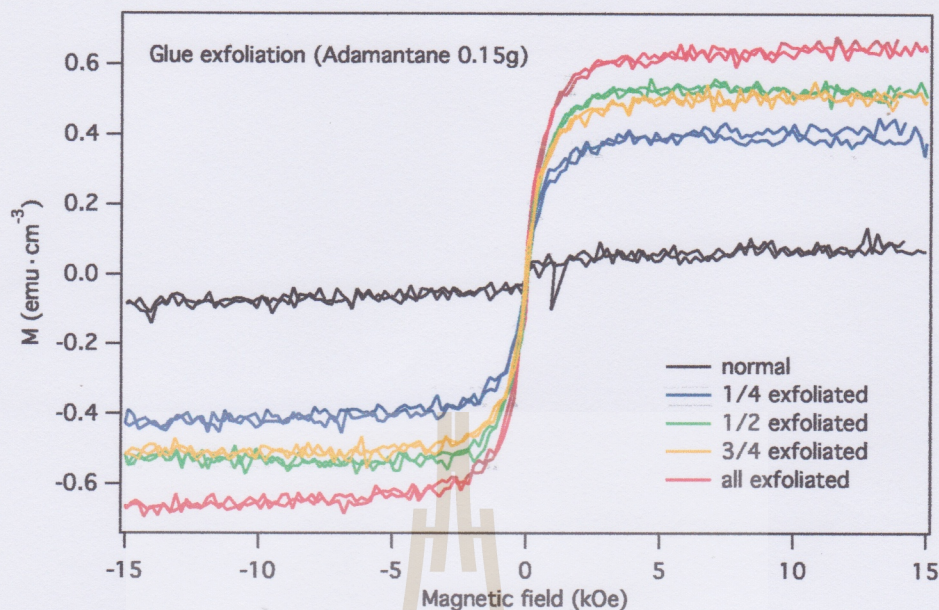
Figure 4.8 M-H curves of exfoliated ferromagnetism in CVD-carbon film, compared to normal CVD-carbon films. The saturated magnetization is higher than the original film by 8.4 times.

4.5.2 Light radiation effect

I also studied light effect on ferromagnetism in CVD-carbon film. In this work, I used green laser irradiated on CVD-carbon film. Figure 4.9 shows M-H curves of ferromagnetism in CVD-carbon film after laser irradiation. The saturation magnetization slightly increases to the highest saturation magnetization is larger than 7.8% (yellow line), compared to the untreated one (black line). However, the saturation magnetization will go down to the original one when I closed laser and left a sample for a couple hours in atmosphere. This result is supported by the changes of D-peak of Raman spectra after laser irradiation in Figure 4.7 that disordered peak was change after irradiation.
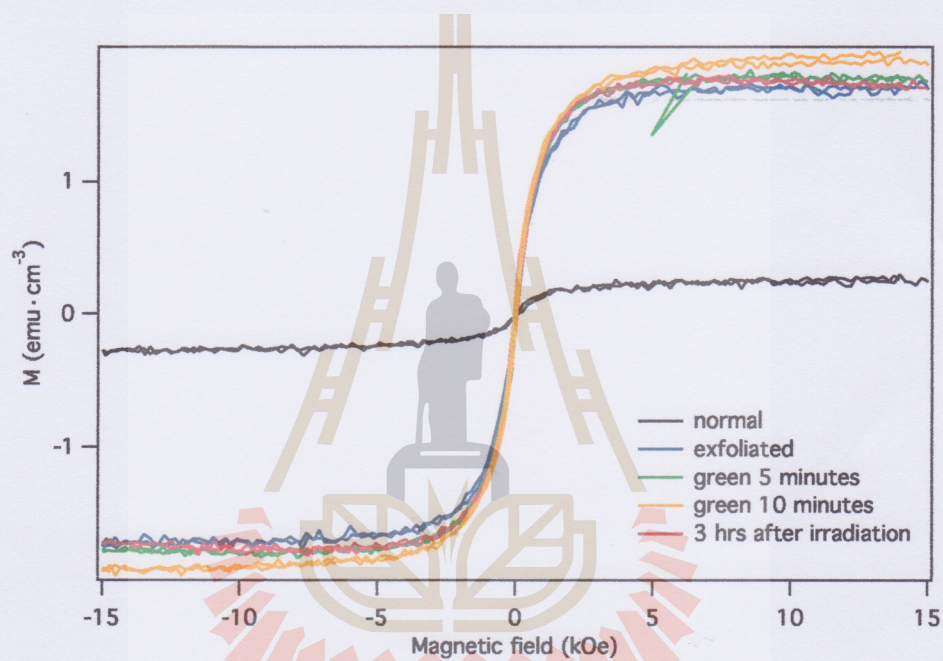
Figure 4.9 M-H curves of CVD-carbon film, after laser irradiation. Saturation magnetization slightly enhances after irradiation. However it goes down after closed irradiation

CHAPTER V

SUMMARY AND FUTURE DIRECTION

5.1 Summary of the ferromagnetism studies

In summary, we report moderately strong ferromagnetism in CVD-carbon films prepared by using adamantane powders as precursor. This ferromagnetic behavior are mixed together with diamagnetic signal which is from the quartz substrate. After diamagnetic background subtraction, the saturated magnetization is found to be as large as $6.2 \ emu \cdot cm^{-3}$. If we assume that the density of our film will be the same of density of graphite which is around $3 \ g \cdot cm^{-3}$, its saturation magnetization will be around $2.06 \ emu \cdot g^{-1}$. This is quite strong magnetizations since compared to the teflon which is around $2.5 \ memu \cdot g^{-1}$ (Ma et al., 2012). The saturated magnetization is increased when temperature is decreased, indicating the characteristics of magnetic material. The possibility of having magnetic metals impurities as the main cause is ruled out since the amount needed to explain the observed magnitude (e.g. 1% of Fe) could not be detected be energy dispersive x-ray spectroscopy (with sensitivity of 1000 ppm). Importantly, by using vibrating sample magnetometer, the saturation magnetization is further enhanced as large as 8.4 times after mechanically exfoliation. In addition, the saturation also slightly increases after laser irradiation.

Since the other studies proposed that the origin of ferromagnetism in carbon based material could be structural defect as dangling bond, the Raman spectra exhibits the various carbon bondings, including sp^2, sp^3, and C-H bonds. Since adamantane is only sp^3, dangling bonds may be created after some carbon bond

was broken in CVD-process. To further observe the effect of laser irradiation, the Raman found the changes of carbon structure after shining green laser.

5.2 Future direction

Although ferromagnetism of CVD-carbon film is much higher than Teflon study, it is still be enhanced since its saturation magnetization is around 1% of Fe ($220 \; emu \cdot g^{-1}$). I would like to optimize parameter for increasing ferromagnetism such as adamantane precursor and operating temperature. In Telapatra et al., study, they induced ferromagnetic signal by using nitrogen ion bombardment on nanosized diamond (Talapatra et al., 2005). Then I would like to prepared CVD-film under N_2 atmosphere. In medical view, they used magnetic nano particle for transporting and releasing drug in human's body. We believe that our CVD-film can be replaced the magnetic nano particle since it is inexpensive and more bio-compatible than magnetic particle.

REFERENCES

REFERENCES

Andriotis, N., Menon, M., Sheetz, R., and Chernozatonskii, L. (2003). Magnetic properties of C60 polymers. **Phys. Rev. Lett.** 90: 26801.

Coey, J. (2005). D0 ferromagnetism. **Solid. State. Sci.** 7: 660.

Esquinazi, P., Setzer, A., Höhne, R., Semmelhack, C., Kopelevich, Y., Spemann, D., Butz, T., Kohlstrunk, B., and Lösche, M. (2002). Ferromagnetism in oriented graphite samples. **Phys. Rev. B** 66: 024429.

Esquinazi, P., Spemann, D., Höhne, R., Setzer, A., Han, K.-H., and Butz, T. (2003). Induced magnetic ordering by protron irradiation in graphite. **Phys. Rev. Lett.** 91: 227201.

Friedman, A., Chun, H., Jung, Y., Heiman, D., Glaser, E., and Menon, L. (2010). Possible Room Temperature Ferromagnetism in Hydrogenated Carbon Nanotubes. **Phys. Rev. B** 81: 115461.

George, T. F., Zhang, G., Mansoori, G. A., and Assoufid, L. (2007). Diamondoids in nanotechnology First-principles simulation of electronic structure and nonlinear optical response. **IEEE**.

Han, K. H., Spemann, D., Esquinazi, P., Höhne, R., Riede, V., and Butz, T. (2003). Ferromagnetic spots in graphite produced by proton irradiation. **Adv. Mater.** 15: 1719.

Kim, J. H., Choi, J., Chang, K., and Tománek, D. (2003). Defective fullerenes and nanotubes as molecular magnets:An ab initio study. **Phys. Rev. B** 68: 125420.

Lehtinen, P. O., Foster, A. S., Ma, Y., Krasheninnikov, A. V., and Nieminen, R. M. (2004). Irradiation-induced magnetism in graphite: A density functional study. **Phys. Rev. Lett.** 93: 107202.

Ma, Y. W., Lu, Y. H., Yi, J. B., Feng, Y. P., Herng,.T. S., Liu, X., Gao, D. Q., Xue, D. S., Xue, J. M., Ouyang, J. Y., and Ding, J. (2012). Room temperature ferromagnetism in Teflon due to carbon dangling bonds. **Nat. Commun.** 3: 727.

Makarova, T., Sundqvist, B., Höhne, R., Esquinazi, P., Kopelevich, Y., Scharff, P., Davydov, V., Kashevarova, L. S., and Rakhmanina, A. V. (2001). Magnetic carbon. **Nature** 413: 716.

Mansoori, G. A. (2007). Diamondoid molecules. **Adv. Chem. Phys.** 136: 207.

Meevasana, W., Supruangnet, R., Nakajima, H., Topon, O., Amornkitbamrung, V., and Songsiriritthigul, P. (2009). Electron affinity study of adamantane on Si(111). **Appl. Surf. Sci.** 256: 934.

Moriguchi, H., Ohara, H., and Tsujioka, M. (2016). History and applications of diamond-like carbon manufacturing processes. **SEI Technical Review**: 52.

Narasimha, K. T., Ge, C., Fabbri, J. D., Clay, W., Tkachenko, B. A., Fokin, A. A., Schreiner, P. R., Dahl, J. E., Carlson, R. M. K., Shen, Z. X., and Melosh, N. A. (2016). Ultralow effective work function surfaces using diamondoid monolayers. **Nat. Nanotechnol** 11: 267.

Ohldag, H., Esquinazi, P., Arenholz, E., Spemann, D., Rothermel, M., Setzer, A., and Butz, T. (2010). The role of hydrogen in room-temperature ferromagnetism at graphite surfaces. **New. J. Phys** 12: 123012.

Ohldag, H., Tyliszczak, T., Höhne, R., Spemann, D., Esquinazi, P., Ungureanu, M., and Butz, T. (2007). Pi-electron ferromagnetism in metal-free carbon probed by soft x-ray dichroism. **Phys. Rev. Lett.** 98: 187204.

Ramezani, H. and Mansoori, G. A. (2007). Diamondoids as molecular building blocks for nanotechnology. 109:44.

Robertson, J. (2002). Diamond-like amorphous carbon. **Mater. Sci. Eng. R Rep.** 37: 129.

Saito, T., Nishio-Hamane, D., Yoshii, S., and Nojima, T. (2011). Ferromagnetic carbon materials prepared from polyacrylonitrile. **Appl. Phys. Lett.** 98: 052506.

Saito, T., Ozeki, T., and Terashima, K. (2005). Magnetism in diamond-like carbon. **Solid. State. Comun.** 136: 546.

Siriroj, S., Lowpa, S., Dahl, J. E. P., Sangphet, S., Doonyapisut, D., Uppachai, P., Eknapakul, T., Jaiban, P., Prachumrak, N., Bawden, L., Nakajima, H., Supruangnet, R., Delinger, J., Sudyoadsuk, T., Promarak, V., Songsiritthigul, P., Kundhikanjana, W., Maensiri, S., Melosh, N. A., King, P. D. C., Shen, Z. X., Pimanpang, S., and Meevasana, W. (2016). Diamondoid electrode as an alternative to high-performance platinum electrode in dye-sensitized solar cell.

Sriplai, N., Pinitsoomtorn, S., Chompoosor, A., Amnuaypanich, S., Maensiri, S., and Amornkitbamrung, V. (2015). Ferromagnetism in Metal-Free Polymers. **IEEE Magn. Lett.** 6: 1000104.

Talapatra, S., Ganesan, P. G., Kim, T., Vajtai, R., Huang, M., Shima, M., Ramanath, G., Srivastava, D., Deevi, S. C., and Ajayan, P. M. (2005).

Irradiation-induced magnetism in carbon nanostructures. **Phys. Rev. Lett.** 95: 097201.

Ugeda, M. M., Brihuega, I., Guinea, F., and Gómez-Rodr´iguez, J. M. (2010). Missing atom as a source of carbon magnetism. **Phys. Rev. Lett.** 104: 96804.

Wang, Y., Huang, Y., Song, Y., Zhang, H., Ma, Y., Liang, J., and Chen, Y. (2009). Room-Temperature Ferromagnetism of Graphene. **Nano. Lett.** 9: 220.

Wood, R. A., Lewis, M., Lees, M., Bennington, S. M., Cain, M. G., and Kitamura, N. (2002). Ferromagnetic fullerene. **J. Phys. Condens. Matter** 14: 385.

Xia, H., Li, W., Song, Y., Yang, X., Liu, X., Zhao, M., Xia, Y., Song, C., Wang, T. W., Zhu, D., Gong, J., and Zhu, Z. (2008). Tunable magnetism in carbon-ion-implanted highly oriented pyrolytic graphite. **Adv. Mater.** 20: 4679.

Yang, W. L., Fabbri, J. D., Willey, T. M., Lee, J. R. I., Dahl, J. E., Carlson, R. M. K., Schreiner, P. R., Fokin, A. A., Tkachenko, B. A., Fokin, N. A., Meevasana, W., Mannella, N., Tanaka, K., Zhou, X. J., Buuren, T. V., Kelly, M. A., Hussain, Z., Melosh, N. A., and Shen, Z. X. (2007). Monochromatic electron photoemission from diamondoid monolayers. **Science** 316: 1460.

Yang, X., Xia, H., Qin, X., Li, W., Dia, Y., Liu, X., Zhao, M., Xia, Y., Yan, S., and Wang, B. (2009). Correlation between the vacancy defects and ferromagnetism in graphite. **Carbon** 47: 1399.

Yazyev, O. and Helm, L. (2007). Defect-induced magnetism in graphene. **Phys. Rev. B** 75: 125408.

Zanolli, Z. and Charlier, J. (2010). Spin transport in carbon nanotubes with magnetic vacancy-defects. **Phys. Rev. B** 81: 165406.

Zhang, Y., Talapatra, S., Kar, S., Vajtai, R., Nayak, S. K., and Ajayan, P. M. (2007). First-principles study of defect-induced magnetism in carbon. **Phys. Rev. Lett.** 99: 107201.

CURRICULUM VITAE

NAME	Mr. Suppanut Sangphet
DATE OF BIRTH	March 24, 1994
PLACE OF BIRTH	Surin, Thailand
PERSONAL ADDRESS	105/9 Phorang Rd., Thumbol Naimuang, Muang
	District, Surin 32000, Thailand
	Mobile. 66-90-6107075
E-MAIL	suppanut.tone@gmail.com

EDUCATIONS

MsC candidate (2016 - present)

School of Physics, Suranaree University of Technology, Nakhon Ratchasima, Thailand

Title of Thesis: Study of origin and enhancement of room-temperature ferromagnetism in CVD-carbon films prepared by using adamantane as presursor

Supervisor: Asst. Prof. Dr. Worawat Meevasana

Bachelor of Science (2013 - 2016)

School of Physics, Suranaree University of Technology, Nakhon Ratchasima, Thailand

Advisor: Asst. Prof. Dr. Worawat Meevasana